Do upwelled waters from the California Undercurrent contribute to high pCO_2 within the fjord system of Nootka Sound, BC?

Genevieve Hinde

University of Washington,
School of Oceanography,
Box 35790,
Seattle,
WA 98195-5060
gjgh1n12@soton.ac.uk

Advised by Jim Murray and Julian Sachs

Acknowledgements

I would like to thank my advisors Jim Murray and Julian Sachs for their guidance on my project and Arthur Nowell for guiding me through the writing process. I would particularly like to thank all those in the Gagnon Lab, including Alex Gagnon, Anne Gothmann and Isaiah Bolden who gave up a lot of their time to train and supervise me for the analysis needed. I would also like to thank all the students and faculty who helped in sample collection during the cruise, particularly Daryn White who I worked in close collaboration with throughout sampling and analysis, and Kathy Newell who ensured we had all the equipment needed. Lastly, thank you to the crew of the R/V Thomas G. Thompson without whom this cruise would not have been possible, and to School of Oceanography for giving me this opportunity.

Abstract

An understanding of coastal ocean-atmosphere CO_2 exchange is important for modelling future greenhouse gas scenarios. This study focuses on the fjord system of Nootka Sound in December 2015. 16 stations were sampled from 60km offshore to the head of Muchalat Inlet with the aim of evaluating the influence of nutrient rich, high pCO_2 waters from the California Undercurrent on the fjord system. Samples were taken throughout the water column to obtain oxygen, nutrient and carbonate system data. Net autotrophy and high nutrient waters were observed at the mouth of the fjord system; though it was thought these waters did not originate from the California Undercurrent as isopycnals were suggestive of coastal downwelling. Deep waters in the fjord had pCO_2> 1500µatm and high levels of denitrification were observed. Higher pCO_2 was observed in surface water compared to the atmosphere at most stations, indicating the fjord was acting as a source of atmospheric CO_2.

Introduction

The study of the carbonate system is key to improving our understanding of ocean acidification, and the buffering effect the oceans have on the concentration of atmospheric CO_2. Atmospheric levels of CO_2 have risen from approximately 280ppm in 1750 to a global average of over 400ppm today (www.esrl.noaa.gov). As a whole the oceans act as a sink for atmospheric CO_2, via the biological pump and the solubility pump. Sabine *et al.* (2005) calculated that without the oceans acting at a carbon sink, atmospheric CO_2 levels would be 55ppm greater than what we observe today.

However, this air-sea CO_2 flux has high spatial heterogeneity, with parts of the ocean, such as the eastern equatorial Pacific, acting as a CO_2 source and other regions, such as the Southern Ocean, acting as a sink (Takahashi *et al.,* 2002). In the open ocean the temperature of the water is both an indicator and a control of CO_2 flux, with cooler waters having an increased solubility of CO_2, whilst also indicating older, upwelled water. Christensen (1994) showed that these upwelled waters often have higher ratios of DIC/Alkalinity and higher partial pressures of CO_2 (pCO_2), and so can act as sources of atmospheric CO_2.

Though continental margins are disproportionately small when compared to the area of the open ocean, their high biological activity, due to an input of nutrients from terrestrial sources and coastal upwelling, means their role in the biological carbon cycle can be significant (Borges and Chen, 2009). Borges (2005) showed that by considering estuary and salt-marsh environments separately from the more general coastal area, the potential carbon sink increased. This demonstrates the importance of understanding the processes controlling CO_2 flux within estuarine systems. With better understanding, we will be able to more accurately model how anthropogenic CO_2 emissions influence the level of CO_2 in the atmosphere and therefore better predict future climate change.

The relationship between river input and offshore input to a fjord system can be complex, due to large seasonal variations in river fluxes and wind forcing, but a major control on the biochemical processes within the fjord system. An extensive study of air-sea CO_2 fluxes was carried out in the Patagonian fjords and Chilean offshore waters by Torres *et al.* (2011). Using data spanning from 1996 to 2009, they found that during summer the Southern Patagonian fjords were a sink for atmospheric CO_2, but in winter, surface waters were often supersaturated in CO_2. High spatial heterogeneity was observed in surface pCO_2 with values increasing towards the mouth of the fjord. Waters above the warm halocline had lower pCO_2 values than those below; this was thought to be a result of net autotrophy in the surface waters. They also observed outgassing of CO_2 in areas where coastally upwelled waters were present.

This study takes place in Nootka Sound, a temperate fjord system on the west coast of Vancouver Island, Canada. The estuary consists of three inner fjords, Tahsis, Tlupana and Muchalat, and an outer fjord area with two main channels around Bligh Island leading to the outer sill and the open ocean. This study focuses on the outer fjord system of Nootka Sound and the Zuciarte Channel. Similarities can be drawn between Nootka Sound and the Patagonian fjord systems, though they are in different hemispheres they are at similar latitudes, both in temperate regions.

As shown by Torres *et al*. (2011), the origin of water in contact with the atmosphere has a large influence on its potential to create an efflux or influx of CO_2 from the atmosphere to the ocean. The California Undercurrent (CU) can be observed off the coast of Vancouver Island (Thomson and Krassovski, 2010) .This is a poleward undercurrent containing Pacific Equatorial Water which is characterised by relatively high temperature and salinity, low dissolved oxygen concentration and high nutrient content (Huyer *et al.,* 1998). Coastal waters off Vancouver Island experience seasonal upwelling due to local wind forcing and shelf waves (Freeland and Denman*,* 1982). Coastal upwelling in this region occurs in spring and summer, however there is still the potential for this deep water to be present in surface waters in winter. Thomson and Krassovski (2010) found that water from the CU entered the Juan

de Fuca Strait (to the south of Vancouver Island) as part of deep estuarine inflow, then gradually mixed into the outflow water. They found that this high nutrient outflow water could be detected off the west coast of Vancouver Island.

A previous study in Nootka Sound by Knox (2015), characterised the surface waters of Muchalat and Tahsis as CO_2 sinks during December, with fluxes of -4.7 $mmolCm^{-2}d^{-1}$ and -1.7 $mmolCm^{-2}d^{-1}$, respectively. It was concluded that surface waters of the inner fjord systems were dominated by the high river fluxes characteristic of Vancouver Island in winter months. Koehlinger (2015) studied the water masses present within the fjord system, she identified offshore influences on water masses within the fjord system but did not chemically characterise these masses.

Upwelled waters also have the potential to influence the carbonate system by supplying nutrients to stimulate primary production. High nutrient waters from the California Undercurrent were observed at Friday Harbour Labs in the San Juan Islands to the south of Vancouver Island, but were not associated with high chlorophyll levels. It was thought that primary production was instead limited by mixing to depths below the photic zone (Murray *et al.,* 2015).

This study investigates the vertical and horizontal distribution of pCO_2 within the outer fjord of Nootka Sound. Chemical and physical parameters including, temperature, salinity, nutrient and oxygen content and carbonate chemistry are used to evaluate the contribution of offshore CU waters to this system.

Methods

Sampling Locations

Sampling was undertaken in Nootka Sound, BC, Canada during the TN334 student cruise on-board R/V Thomas G. Thompson, 10-20 December 2015. Data was collected at 16 stations which formed a transect from approximately 60km offshore on the shelf break, to the head of Muchalat Inlet (Figure 1). At each station a full CTD profile was taken and water samples were collected for analysis of nutrients, oxygen, dissolved inorganic carbon (DIC) and alkalinity. A minimum of 5 water samples were taken at each station within the fjord system. Depths were chosen as surface (~2m), within the surface mixed layer, just above the thermocline, just below the thermocline, and 10m above the bottom (bottle locations are shown on figures where relevant). At some stations additional samples were taken and at the shallow stations U02 and U03, only 2 and 3 samples were taken respectively. Locations and dates of sampling can be found in Table 1. Station 'Nootkaend' and station 'Offshore' have the same location, however were occupied 1 week apart. Water samples were taken when the station was first occupied ('Nootkaend') and all profile data was used from when the station was reoccupied ('Offshore'). This was because it was thought that some of the sensors were not reading accurately on the initial cast.

Station Name	Latitude (°)	Longitude (°)	Date (DD/MM/YYYY)	Time GMT (PST+8)	Tidal State
Nootkaend	49.0005	-127.1053	12/12/2015	04:31- 05:47	High
Offshore	48.99852	-127.10466	19/12/2015	16:15	End of ebb
U04	49.10906	-127.06302	19/12/2015	13:51	Mid ebb
U03	49.36798	-126.9314	19/12/2015	11:24	High
U02	49.51954	-126.7189	19/12/2015	09:34-09:48	End of flood
C1	49.56488	-126.62766	12/12/2015	11:31-11:46	Low
C2	49.58652	-126.59764	12/12/2015	12:52-13:21	Start of flood
C3	49.59806	-126.58349	12/12/2015	14:36-15:04	Mid flood
C4	49.60221	-126.5227	12/12/2015	15:59-16:25	Mid flood
C5	49.63202	-126.49648	16/12/2015	09:48-10:15	Mid ebb
C6	49.64492	-126.44742	16/12/2015	13:48-14:09	Low
C7	49.64842	-126.3723	12/12/2015	Hrs before C8	End of Ebb
C8	49.64398	-126.30034	13/12/2015	00:07-00:47	Start of flood
C9	49.65926	-126.2225	13/12/2015	04:32-05:39	High
C10	49.66724	-126.14274	13/12/2015	09:33-10:11	Mid ebb
C11	49.6384	-126.08744	13/12/2015	16:55-17:24	Start of ebb
U01	49.61986	-126.05654	13/12/2015	19:01-19:27	Mid ebb

Table 1 – A table containing locations and timings of all stations used within the project. Tidal data obtained from www.tides.gc.ca. For tide times and amplitudes see Table 4.

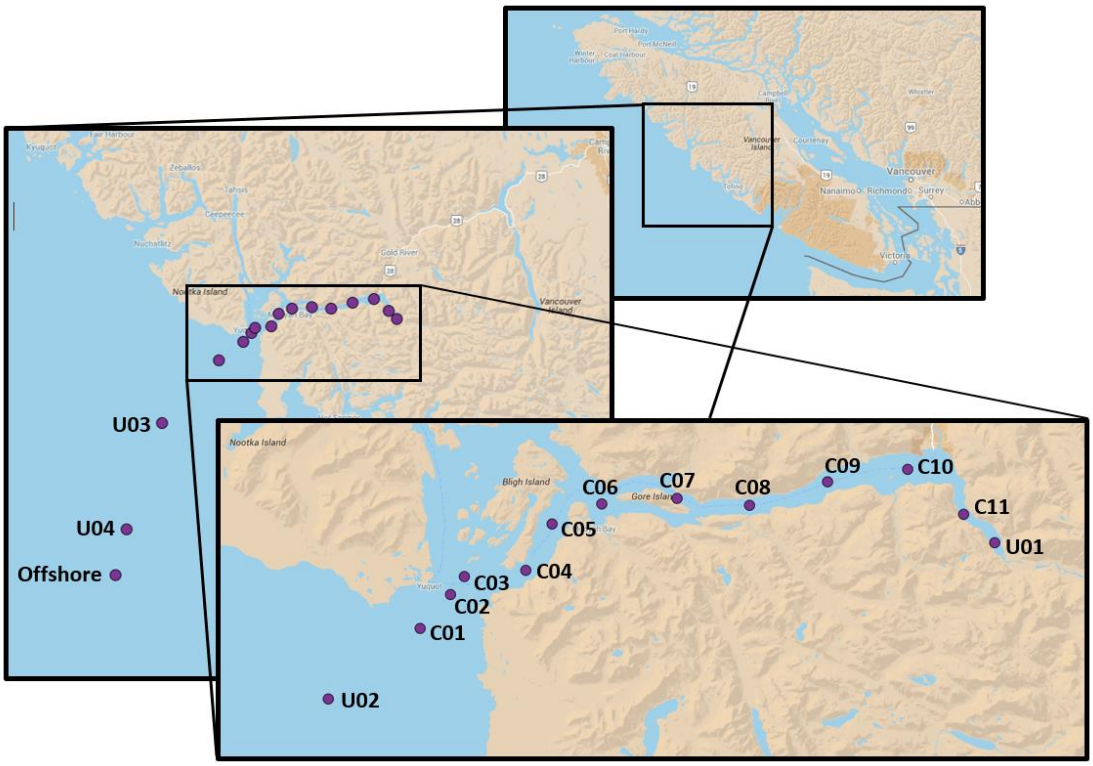

Figure 1- Maps (orientated northwards) showing station locations. In the text, C06 east through U01 are described as Muchalat Inlet, C04 and C05 are within the Zuciarte Chanel (to the south of Bligh Island), C01, C02 and C03 are described as 'Outer Nootka Sound', U02 is at the shallowest depth and U03 in on the continental shelf. U04 and 'Offshore' stations are at different depths on the shelf break. The mouth of the Gold River can be seen north of C10. Map Data: Google 2016.

DIC and Alkalinity

Water samples were collected in 500ml glass ground stoppered bottles for analysis of DIC and alkalinity on return to the University of Washington. Each bottle was filled to minimise contact with the atmosphere using methods as described by SOP 1 (Dickson *et al.,* 2007). Samples were poisoned with 200µL mercuric chloride ($HgCl_2$) to inhibit biological activity, sealed with Apeizion M grease and lids were secured with electrical tape. A small air bubble was left within the neck of each bottle to allow for thermal expansion. Samples were analysed within 1- 4 months of returning to the University of Washington in the Gagnon Lab. Samples were analysed for DIC using a Marianda VINDTA 3D system according to the coulormetric method as described in SOP 2 (Dickson *et al.,* 2007). Alkalinity was measured within 5 days (normally 2) of each bottle being exposed to the atmosphere, using an open cell

Dickon Total Alkalinity Titration System (version 2.9i_1.0) according to the Gran titration method described in SOP 3 (Dickson *et al.,* 2007). Dickson seawater certified reference materials (CRMs) were analysed alongside samples, and used to make daily corrections.

Oxygen

Water samples were collected in 125ml glass stoppered bottles. The same method of filling was used as for the DIC/alkalinity samples to minimise contact with the atmosphere. 1 ml $MnCl_2$ and 1 ml NaOH-NaI solution was added to the sample before the bottle was stoppered and inverted. Samples were analysed on-board R/V Thomas G. Thompson using the Winkler titration method (Carpenter, 1978) using a Metrohm Dosimat 685 titrator. Samples were mostly analysed within 24hrs of collection, however due to many samples being taken in a short space of time, a small backlog was created and so some samples were not analysed until ~2 days after collection. Oxygen data was also collected using an SBE 43 oxygen sensor on the CTD rosette.

Nutrients

Water samples were collected and analysed for nutrient concentration at the Marine Chemistry Lab, School of Oceanography, University of Washington. 45-50ml of sample was filtered using a 60ml syringe and 25mm, 0.45µm pore size Nalgene filter, into a 60 ml HDPE plastic bottle. Space was left at the top of the bottle to allow for expansion and samples were stored at -10°C for the remainder of the cruise. Each sample of water collected was analysed for nitrate (NO_3^-), nitrite (NO_3^{2-}), ammonia (NH_3), phosphate (PO_4^{3-}) and silicate ($SiOH_4^{2-}$).

Chlorophyll

Chlorophyll samples were collected from the near surface (~2m) depth at the 5 stations in Nootka Sound and the Zuciarte Channel. Samples were refrigerated in dark containers and filtered within 24hrs using a vacuum filtration system through a glass fibre filter (GFF). The filter paper was retained and

analysed using a fluorometer (Turner TD700) according to methods initially described by Lorenzen (1967).

Physical parameters

Temperature, salinity and pressure data was obtained from the Seabird (SBE 911plus) CTD. Density calculated within the CTD program, was used when converting moles per volume to moles per mass.

pCO_2

The partial pressure of CO_2 within each water sample was calculated from DIC and alkalinity, and used salinity, temperature and pressure data obtained from the CTD. The CO2SYS version 1.1 toolbox was used in MatLab to calculate pCO_2. For this calculation the Mehrbach (refit by Dickson and Millero) K1 and K2 constants (Dickson and Millero, 1987) were used, the Dickson KSO4 dissociation constant (Dickson, 1990) and the TB (borate to salinity ratio) of Lee *et al*. (2010) was used. Atmospheric CO_2 data was obtained through Environment Canada. This data was available at hourly intervals at Estevan Point (49°35'N, 126°22'W), which lies approximately 20km south of the entrance to Nootka Sound.

AOU

Apparent oxygen utilisation (AOU) was calculated by subtracting measured oxygen concentration from the theoretical saturated concentration. Saturated oxygen concentrations were calculated using the gsw_O2sol_SP_pt function from the Gibbs seawater toolbox in MatLab, with salinity and potential temperature data from the CTD casts. Where possible measured oxygen concentrations were used from the Winkler titrations, however in the absence of the data, corrected oxygen data from the optode was used (see figure legends for details on each plot).

Surface Salinities

Due to the strong stratification within the surface 3m of the water column within the fjord, it was thought that the salinities for bottle samples obtained from the CTD data may not have given an accurate representation of the salinity of the sample. For two stations (C7 and C8) there was no salinity

data at the surface bottle depth. The salinity of all surface samples obtained from the CTD rosette within the fjord was re-measured using a refractometer. A more accurate form of analysis was not used due to limitations with the volume of water available for testing, and that that water available was poisoned with mercuric chloride. Values obtained using the refractometer were compared to those obtained from the CTD, for the two stations where no CTD data was available or where there was a disagreement of more than 2.5 salinity units, salinities obtained using the refractometer were used in calculations regarding the bottle samples.

Results

Density, Salinity and Temperature

Within Muchalat Inlet and Zuciarte Channel a strong density structure was observed with a light fresh layer within the surface 1m and a range of >4kgm^{-3} seen within the upper 50m of the water column near the mouth of the Gold River. Deep water within Muchalat Inlet and the Zuciarte Channel had densities of 1025-1026kgm^{-3}. Looking at Figure 2, you can observe sloping isopycnals at the entrance to the fjord system, offshore waters reach densities >1027kgm^{-3} below 600m. Water of a density of 1026.5kgm^{-3} which is thought to correspond to the California Undercurrent was seen at a depth of 200m offshore. Surface waters within Muchalat were around 10°C (Figure 3), with a temperature maximum of 13.2°C seen at a depth of 30m at the head of Muchalat inlet, a signature of this maximum was seen throughout Muchalat Inlet, decreasing towards the mouth. Temperatures within the deeper layers of Muchalat Inlet were all close to 8°C with a very slight warming in the deep waters of the Zuciarte Channel. The surface 60m of offshore water also had temperatures of 10°C, with temperatures then decreasing with depth to a temperature of 2.1°C at the 1640m.

Salinities of 34.5 were observed at depths of 1640m offshore. Large variation was observed in salinity in the upper layers of Muchalat Inlet (Figure 4), with the lowest salinity of 5 observed in the surface waters of C08. Salinities lower than these may have been observed if samples above 1m were able to be

sampled from the CTD. The majority of waters below the surface layers within the fjord system had salinities of 33. Figure 6 shows 4 stations in T-S space, and indicates large variation in T-S signatures between offshore, shelf and within inlet waters.

Nutrients

Ammonia (Figure 7) levels within Muchalat inlet were low with near 0$\mu molkg^{-1}$ concentrations in the deep waters and concentrations of ~0.2$\mu molkg^{-1}$ within waters above the 1024.5kgm^{-3} isopycncal. Within Zuciarte Channel higher concentrations of up to 1$\mu molkg^{-1}$ were observed in surface waters, and waters above 0$\mu molkg^{-1}$ were observed in the full water column over the sill at the entrance to Nootka Sound. Concentrations were also low in offshore waters though slightly elevated concentrations of ~0.5$\mu molkg^{-1}$ were observed at depths of 75m and 250m.

Nitrite (Figure 8) showed a similar distribution to ammonia with near 0$\mu molkg^{-1}$ in the majority of the inlet. Higher concentrations of ~0.5$\mu molkg^{-1}$ were observed in the water column over the sill and traces of these elevated concentrations appeared throughout the surface 50m of the Zuciarte Channel. Offshore, near 0$\mu molkg^{-1}$ concentrations were observed at all depths except within the surface 75m which showed concentrations of ~0.2$\mu molkg^{-1}$.

High concentrations of nitrate were seen in the deep waters offshore (Figure 9), they ranged from 42.4$\mu molkg^{-1}$at 1387m to 24.4$\mu molkg^{-1}$ at 168m. Similar concentrations were seen within the surface 100m inside and outside of the fjord system. Nitrate concentrations of 10-15$\mu molkg^{-1}$ were seen in surface waters to a depth of ~50m, and nitrate of 25$\mu molkg^{-1}$ was seen within the fjord system 50m-bottom and offshore 75-150m. Slightly higher concentrations of ~30$\mu molkg^{-1}$ were observed at a depth of ~150m within Zuciarte Channel.

As with nitrate, silicate was shown to be high in deep offshore waters, ranging from 154.9$\mu molkg^{-1}$at 1387m to 33.5$\mu molkg^{-1}$ at a depth of 168m (Figure 10). Concentrations observed within the deep basin

(100m - < 350m) of the inlet (~75µmolkg^{-1}) were higher than offshore concentrations at comparable depth (~30-60µmolkg^{-1}). Similar to nitrate, higher silicate concentrations in comparison to surroundings were observed at depths of ~150m in the Zuciarte Channel. Within the top 50m of the fjord waters, high concentrations (~30µmolkg^{-1}) were observed in surface waters with the lowest concentrations (15-20µmolkg^{-1}) observed deeper at ~10-30m.

Elevated concentrations (3.7 µmolkg^{-}1) compared to surroundings (~2.8 µmolkg^{-1}) at 150m in Zuciarte Channel were also seen in the phosphate data (Figure 11) and higher concentrations were seen within the basin at depths of 100-300m than similar depths offshore. Similar concentrations were seen throughout the Inlet in surface water ranging from ~1µmolkg^{-1} near surface to ~2µmolkg^{-1} at 50m.

N* values of ~15 µmolkg^{-1} were observed in most of the deep waters within Nootka Sound and Muchalat Inlet (Figure 12), with values of -30 µmolkg^{-1} observed locally in the same region as the temperature wedge near U01 at a depth of 75-100m. Within the surface 60m of the fjord system, values were above -5 µmolkg^{-1}. A much smaller range of values was observed offshore (-1.5 to -5 µmolkg^{-1}), a distinct minimum was observed at depths of 150-250m.

The relationship between Nitrogen (N) and Phosphorus (P) can be seen in Figure 13. Offshore waters are observed to have an N:P similar to that of the Redfield (Redfield *et al*., 1963) ratio but being limited by N at P < 0.5µmolkg^{-1} . Data from within the fjord system appears to lie on a line with gradient 7:1.

Chlorophyll and Fluorescence

Surface chlorophyll data from the station within Nootka Sound show chlorophyll concentrations ranging from 0.013µgL^{-1}at C5 to 0.266µgL^{-1} at C3. Replicates of chlorophyll concentration had a large range of 0.175µgL^{-1} and correlation of sample chlorophyll data with fluorescence at the same depth was poor (Figure 14) with an R^2 value of 0.2331 when a linear polynomial was fitted. It is thought this poor

correlation was a result of inconsistent chlorophyll sample collection methods, and fluorescence data being taken from a different depth as the sample. This difference in depth may have resulted from the fluorometer being located approximately 0.5-1.5m below the depth of the sample bottle. It may have also resulted from a lack of data in the surface 2-3m of the water column.

A transect of fluorescence is shown in Figure 15 and shows the highest levels of fluorescence over the shelf and in off-shelf waters above 80m, and lower levels of fluorescence at the entrance to Nootka Sound and into the Zuciarte channel. Below 80m in the open water and within Muchalat Inlet negligible levels of fluorescence were observed.

Turbidity

Light transmission (Figure 16) was near 100% in most regions, however decreased to 85% over the continental shelf and was seen at transmission <60% in surface and deep waters within the entrance to Nootka Sound. Low light transmissions of around 90% were also observed at near bottom depths within Muchalat Inlet.

Oxygen and AOU

Figure 17 shows waters below the surface mixed 50m, to be low in oxygen with concentrations <100 $\mu molkg^{-1}$, concentrations this low offshore were not seen until below a depth of 400m. Surface waters were high in oxygen with the highest concentrations of 270$\mu molkg^{-1}$ observed in the surface waters of the Zuciarte channel. AOU within Muchalat Inlet (Figure 18) ranged from ~250$\mu molkg^{-1}$ in the deep waters (50-300m) to negative values in the surface 10m of the seaward end of Zuciarte Channel. Waters over the outer sill and continental shelf also showed values close to 0 $\mu molkg^{-1}$.

Figure 19 shows the relationship of AOU to nitrate, as with N:P, the data from the offshore station plots along a line with a similar gradient to the Redfield ratio (Redfield *et al*., 1963). Data from within the inlet has more scatter in the denser waters but a general pattern can be seen of greater changes in AOU

for the change in nitrate than predicted by either the Redfield (Redfield *et al*., 1963) or Hedges (Hedges *et al*., 2002) ratios.

DIC, Alkalinity and pCO_2

Figures 20 and 21 show the freshwater input of the Gold River to be a strong control on Alkalinity and DIC with concentrations <1000 $\mu molkg^{-1}$ in surface waters within Muchalat and ~2000 $\mu molkg^{-1}$ in the surface waters of Zuciarte Channel for both alkalinity and DIC. Alkalinity and DIC appear to be reasonably homogenous at ~2500 $\mu molkg^{-1}$ within the deep waters of the fjord system. Offshore (Figure 22) at the surface, alkalinity is higher than DIC by 160$\mu molkg^{-1}$, both increase with depth and the concentration of DIC surpasses alkalinity at a depth of 440m.

Extremely high pCO_2 is seen within Muchalat Inlet (Figure 23) and the Zuciarte Channel with the highest values of ~2200µatm at 100m depth at the head of Muchalat Inlet and 150m deep within the centre of Zuciarte Channel. Within the surface mixed 50m of the fjord system pCO_2 ranged from ~400-800µatm. Offshore surface values were 393.3µatm at surface and increased with depth down to 1361.3µatm at 350m, then decreased down to 1073.4µatm at 1620m. Air- sea gradient of pCO_2 is summarised in Table 2. Differences between pCO_2 in surface waters and in the atmosphere (ocean – atmosphere) ranged from -52.8µatm at C07 to +508.6µatm as C08, though most positive values were nearer 100µatm or lower.

Station	**Offshore**	**C01**	**C02**	**C03**	**C04**	**C05**	**C06**	**C07**	**C08**	**C09**	**C10**	**C11**	**U01**
Sample depth (m)	0.5	3.0	2.2	2.0	2.6	1.3	1.7	2	2	1.6	0.9	1.2	1.2
Ocean pCO_2	392.4 ±17	453.6 ±20	450.7 ±20	397.7 ±18	510.8 ±23	555.5 ±25	488.1 ±22	354.1 ±15	915.1 ±43	486.3 ±22	356.9 ±16	421.8 ±19	877. 0 ±41
Atm pCO_2	406.7	408.2	407.7	406.3	405.1	407.6	407.2	406.9	406.5	406.9	407.3	408.1	408.0
ΔpCO_2 (ocean-atm)	-14.3	+45.4	+43.0	-8.6	+105.7	+103.2	+147.9	-52.8	+508.6	+79.4	-50.4	+13.7	+469.0

Table 2 – Table indicating near surface pCO_2 and air-sea pCO_2 gradient at all stations with samples close to surface. Atmospheric CO_2 data for Estevan Point courtesy of Environment Canada. Depth of bottles at C07 and C08 are reported to 1s.f. due to uncertainties in precise closing depth.

Alkalinity is plotted against DIC in Figure 24. This figure appears to show slightly different relationships between DIC and alkalinity for different densities of water. Offshore waters above a depth of 550m have a Δalkalinity: ΔDIC of 1:2, and below 700m have a ratio of near 1.5:1. Waters below 10m within the fjord system also show to plot on a similar gradient to the above 550m offshore waters (1:2), with waters within the top 10m having a ratio of close to 1:1.

Comparing DIC and alkalinity against salinity (Figure 25) you can observe a linear relationship in all data up to salinities of 34. Comparing the plot of DIC with that of alkalinity the plots appear very similar except that at a salinity of 33 DIC plots slightly off of this line, with the U04 and Offshore stations plotting below the line and stations within Muchalat Inlet and the outer Nootka Sound area plotting above the line. In both alkalinity and DIC at salinities of 34-35 a steeper gradient is observed. Figure 26 and Figure 27 display this salinity normalised data in section view. Normalised alkalinity appears to be fairly constant over both the upper and lower layer of the fjord at values of ~2375$\mu molkg^{-1}$; the variation in the surface samples is not evaluated as this is likely a feature of inaccuracies in salinity as noted previously. Normalised DIC shows more variation, with the upper fjord waters clearly showing a lower DIC content, by over 100$\mu molkg^{-1}$, compared to the deep waters.

Carbonate Data Uncertainties

Analysis of error for DIC, alkalinity and pCO_2 was approached in two different ways. The first calculated the pooled standard deviation on samples ran in triplicate. DIC used a grouping of 4 triplicates and alkalinity used a grouping of 6 triplicates. This analysis generated a value for 1 standard deviation of 1.49$\mu molkg^{-1}$ DIC and 2.33$\mu molkg^{-1}$ alkalinity.

The second approach utilised an internal lab standard. Two batches of internal standards were used across the period of analysis, the mean DIC value was calculated for each batch using data from all runs. Deviations of individual samples were taken from the relevant mean to calculate the pooled standard deviation. This analysis generated a value for 1 standard deviation of 4.49$\mu molkg^{-1}$ DIC (using a grouping

of 39). Internal standards were not analysed for alkalinity frequently enough to be representative of the dataset, however for comparison (using a grouping of 7) this method generated a standard deviation of 1.31µmolkg^{-1}.

pCO_2 was calculated using the DIC and alkalinity data, however propagation of this error is complex. Hoppe *et al*. (2010) investigated how errors propagate in various calculations of pCO_2. For calculation using DIC and alkalinity assuming an initial uncertainty in both DIC and alkalinity of 5µmolkg^{-1} they found uncertainties in pCO_2 of 7µatm at low pCO_2 (180µatm) and uncertainties of 47µatm at high pCO_2 (1000µatm). Discrepancies in pCO_2 were found to increase proportionally to changing DIC and alkalinity and so for the purpose of this error calculation, errors were calculated using a linear interpolation of the errors established by Hoppe *et al*. (2010). Though the standard deviations generated using the data from this study are less than the 5µmolkg^{-1}, 5µmolkg^{-1} is used as a conservative estimate of error for ease of pCO_2 error calculations.

Discussion

Is outer Nootka sound a source or sink for atmospheric CO_2?

Direction of flux of CO_2 is dependent on the gradient of pCO_2 (ΔpCO_2) between atmosphere and ocean (where $\Delta pCO_2 = pCO_{2ocean} - pCO_{2\,atm}$). A flux of CO_2 into the atmosphere (positive ΔpCO_2) is seen at all stations in the outer Nootka Sound area with the exception of station C03 which showed a small flux of CO_2 into the ocean (Table 2). Biology can be important in steepening or shallowing this gradient. Primary production will act to make the gradient more negative by lowering the pCO_2 of the water; respiration and mixing of high pCO_2 waters to the surface will act to make the gradient more positive.

To evaluate the controls on the gradient, the primary production must be quantified and the pCO_2 of waters supplying the surface waters must be studied. Looking at Figure 18 and Figure 19 negative AOU values can be observed, indicating near surface waters are oversaturated in oxygen. This oversaturation

may be as a result of bubble injection or primary production. Data is not available to evaluate quantitatively how much of this oversaturation is caused by bubble injection, however by looking at the correlation of AOU with other biologically controlled parameters it can be evaluated whether bubble injection is a major control.

Though the accuracy of the chlorophyll data is questionable, no value exceeded 0.3μgL^{-1}, indicating low phytoplankton biomass. However, it must be noted that this may not reflect the carbon fixation of the system, as grazing could be controlling biomass. Fluorescence data cannot be used to give absolute values for primary production, however, it can be used comparatively between stations. By comparing Figure 18 with Figure 15, it can be observed that the areas with positive AOU (outer Nootka Sound and offshore) also show comparatively high fluorescence, hence, it is assumed that primary production is acting to make the pCO_2 gradient more negative in outer Nootka Sound area.

This leads to the question of why these high AOU waters are not observed within the surface waters of Muchalat Inlet. Primary production is known to be commonly limited by two parameters, light intensity and nutrient supply. The majority of stations were occupied during hours of darkness and so a comparison between light compensation depths is not available. However, the controls on the depth of light penetration are insolation and the amount of particulates within the water column. If it is assumed that insolation is constant over the small spatial and temporal scales of the study; the turbidity of surface waters can be compared to determine whether light is limiting primary production. Figure 16 shows stations within Muchalat Inlet to have higher light transmission (lower turbidity) compared to the stations in outer Nootka Sound. This indicates that nutrient supply is likely controlling primary production within the fjord system. It must be noted however that there is no data for the turbidity of the surface 3m; though it is not observed in the data, stations dominated by river inflow may have high turbidity in surface waters. It should also be noted that variable weather was seen over the 10 day period of the study and so the assumption of constant insolation may not hold true.

Of the 5 nutrients studied, transects of ammonium, nitrite and phosphate (Figures 7, 8 and 11) show higher concentrations within the surface mixed layer on the continental shelf and throughout outer Nootka Sound, compared to the surface mixed waters within Muchalat Inlet. This indicates an open water source for the nutrients which appear to stimulate primary production in the outer Nootka Sound area.

Despite this apparent carbon fixation in outer Nootka Sound, efflux was more commonly observed throughout the fjord system (Table 2). The pCO_2 of waters in the surface 60m were in the region of 500µatm. This shows that, even when waters in outer Nootka Sound were net autotrophic, waters at the surface can still have higher pCO_2 than the atmosphere. The deep waters of the fjord have extremely high pCO_2 (> 1500µatm); mixing of deeper fjord waters into the surface layer would allow for ~500µatm pCO_2 in the surface layer. A potential mechanism for this mixing is internal wave breaking.

Where is the CU found?

Thomson and Krassovski (2010) evaluated the poleward extent of the California Undercurrent, a current which carries water, which originates from Pacific Equatorial Water (PEW), northward. Their study included 8 transects from offshore to the coast, which were plotted in temperature – salinity (T-S) space. Figure 5 indicates that water at a depth of just above 200m contains the highest percentage (~40%) of PEW according to its T-S signature. As noted previously, PEW can be characterised as having comparatively low dissolved oxygen concentrations, high nutrient concentrations and high salinity and temperature (Huyer *et al.,* 1998).

Castro *et al*. (2001) evaluated the level of denitrification in CU waters along a zonal transect at 36°20'N using N* and calculated an average N* within CU waters at that latitude of -2.6µmolkg^{-1} ±1.0. From nutrient data collected at the offshore station we observe values of -2.06µmolkg^{-1} and -1.68µmolkg^{-1} at depths of 168m and 247m respectively. This suggests that the CU is observed at the offshore station at a depth between 150-250m which is in agreement with Thomson *et al*. (2010) and who reported the core of the current to be at 150-225m. Water in this depth range corresponds to a density of 1026.3kgm^{-3} to 1026.6kgm^{-3} which is also in agreement with Thomson *et al*. (2010) who found the highest concentrations of PEW along the 1026.55kgm^{-3} density surface. This is also shown in Figure 6 where an inflection in the offshore T-S profile is observed along this isopycnal. Concentrations of nitrate, phosphate and silicate at this depth agreed with the average concentrations determined by Castro *et al*. (2001) for 60-400m depth within the California Undercurrent, however observed oxygen concentrations were much higher (Table 3).

	DIC	**Alk**	**Oxygen**	**NO_3 (µmolkg^{-1})**	**PO_4 (µmolkg^{-1})**	**$Si(OH)_4$ (µmolkg^{-1})**	**Temp (°C)**	**Sal**	**N* (µmolkg^{-1})**	**pCO2 (µatm)**
CU values	2188	-	2.6±1.0 ml/L	27±6	2.2±0.4	35±15	8.9	33.92±0.19	-2.6±1.0	-
This Study	2179 ±5	2242 ±5	160µmolkg^{-1} ±4.8 (3.75 ml/L ±0.1)	24.40±0.15	1.85±0.03	33.47±0.59	8.0	33.85	-2.06 ±0.15	790±37

Table 3 – Summary of values for different parameters within the California Undercurrent (CU) from previous studies and this study. Oxygen and salinity data from this study was used from a depth of 145m, all other values are from a bottle sample at 168m. CU values of nutrients, temperature, salinity and N* were taken from Castro *et al*. (2001). DIC value was taken from Murray *et al*. (2015). Uncertainties in oxygen are ±1 standard deviation as determined from 2 triplicates. Uncertainties in nutrient data are ± the minimum detection limit as published by the Marine Chemistry Lab.

It is clear that offshore waters influence the nutrient system of outer Nootka Sound and here it is proposed that the CU is present at ~60km offshore from Nootka Sound. However it still must be evaluated whether these high nutrient offshore waters are from the CU. The main mechanism by which deeper waters can be brought to the surface in a coastal setting, is via coastal upwelling. During the time of study, downward tilted isopycnals (Figure 2) were observed approaching the coast, suggestive of

downwelling. This is in agreement with the NOAA upwelling index for 48N 125W and 51N 131W during December 2015 (www.pfeg.noaa.gov). The same index provides indication that upwelling is seasonal and normally observed in the summer months. Freeland and Denman (1982) observed upwelling of CU waters to the south of Vancouver Island in summer, however they found that movement of these deeper waters to the surface was aided by the topography in the Strait of Juan de Fuca. There are uncertainties whether water from the depth of CU could be upwelled to the surface waters without the presence of such a topographic feature.

Comparing nutrient concentrations at the entrance to Nootka Sound to the offshore station, can give an indication of the source of offshore waters entering the inlet. Phosphate, silicate and nitrate concentrations within the surface waters of the entrance to Nootka Sound are similar to those in the surface waters over the shelf and offshore station, but lower than in the CU. Ammonium and nitrite concentrations appear to show the opposite, with higher concentration at the entrance to Nootka Sound compared to all depths at the offshore station. This may indicate an input of nutrients from the sediments and the water column over the shelf as opposed to deep offshore waters. Additional evidence for a sedimentary source of these nutrients is the observation that areas where light transmission (Figure 16) is low are the same areas where ammonia and nitrite are high. Though this argument may not be valid within the photic zone as turbidity can also be high due to the presence of biomass.

Waters from the entrance to Nootka Sound plot far from the offshore station waters in T-S space, indicating that even if some of the water has an offshore source it has undergone significant mixing before reaching the entrance to Nootka Sound (Figure 6). The deeper waters within both Muchalat (C10) and outer Nootka Sound (C04) lie close to the T-S signature of offshore waters along the 1025.5kgm^{-3} isopycnal, though they have a more negative AOU. This could indicate that waters within the fjord system originated from offshore water which was brought over the sill during previous upwelling events

and has since had respiration occurring within it to lower the oxygen content. However, the offshore waters that show this T-S signature are above the depth at which the CU is observed. This suggests that an offshore source may come from shallower depths, or if CU waters were a source, significant mixing with warmer fresher waters, would have had to have occurred. There is also the possibility that once upwelled, these waters warmed slightly when they were near the surface.

Silicate concentrations within the deep waters of Muchalat Inlet exceeded those in offshore waters at depths above 450m. Nutrients were not measured in the river during this study but higher silicate concentrations were observed in near surface low salinity waters within the fjord. It was also noted in a previous study in 1933 (Tully, 1937), that the river contained high concentrations of silicate (9×10^3 milligram atoms per L). However, the concentrations in the deep fjord are still over double that observed in the surface waters. One possible explanation for this high concentration is that long residence times of the deep water allow for the accumulation of silicate from silica rich sinking POM (e.g. dead diatoms). Interestingly, the deep waters of the Zuciarte channel have higher concentrations than the deep waters of Muchalat Inlet, the opposite to what would be expected if the silicate originated from the river. This may indicate an offshore influence or may be a result of the basin being shallower, and there being less water to 'dilute' the silica.

What can carbonate data tell us about processes within the fjord?

Comparing the pCO_2 within the fjord system to offshore, it is clear that processes within the fjord system are increasing pCO_2 in the deep fjord basins. The most likely process increasing pCO_2 in the deep basin is respiration. This idea is supported by high AOU within the deep basin waters. If respiration was to occur in an oxic environment you would expect to find N:P ratios consistent with the Redfield ratio (Redfield *et al*., 1963). However we observe a lower ratio of nitrogen to phosphorus (Figure 13) which indicates that nitrate is being utilized as an oxidising agent and the process of denitrification is occurring; this is confirmed by high negative values of N* in the deep basins (Figure 12).

The relationship between alkalinity and DIC (Figure 24) can give us an indication of processes affecting the carbonate system. The deeper waters within the fjord system mostly had ratios of ΔAlkalinity : ΔDIC of 1:2, these larger changes in DIC compared to alkalinity suggest respiration or dissolution of atmospheric CO_2 (Zeebe and Wolf-Gladrow, 2001). As these waters are away from the surface boundary, respiration is the more likely cause of increased DIC and also agrees with the high respiration previously suggested. The 1:2 ratio is also observed at the offshore station in waters above 400m. Below 400m, a ratio of near 1.5:1 is seen which may suggest $CaCO_3$ dissolution.

Studying the relationship between salinity, alkalinity and DIC can also provide evidence for biochemical processes that may be occurring. The riverine endmember for both alkalinity and DIC appeared to plot along the same line as the near surface samples, suggesting that the DIC and alkalinity of near surface waters is largely controlled by mixing with river water. The sections of normalised DIC and alkalinity (Figure 26 and 27) indicated that the spatial patterns of pCO_2 are predominantly controlled by the variability in DIC, as normalised alkalinity appeared constant throughout the fjord system. These large increases in DIC with minimal changes in alkalinity further support the theory of high respiration in the deep fjord waters.

The likely supply of the organic matter allowing for this respiration is summer primary production; though further studies during the summer months would be required to confirm this. A study by Walsh *et al*. (2008) based in multiple fjords in Vancouver Island found sediments to contain high percentages of terrestrial carbon, which may indicate carbon flux to deep waters may not be as seasonal as originally thought.

Limitations of surface pCO_2 flux

In the calculations of ΔpCO_2 it has been assumed that the surface metres of the water column are well mixed and that pCO_2 at the Niskin bottle depth, which ranged from 0.5m-3.0m (Table 2), is

representative of surface pCO_2 concentrations. Considering that the fjord system is strongly influenced by large freshwater input from the Gold River, this assumption may not hold true. Daryn White (pers. comm.) studied surface CO_2 fluxes throughout Muchalat Inlet, and Tahsis Inlet which extends to the north from Nootka Sound. His initial findings indicate that the surface flux is partly dependent on river flow, with an influx of CO_2 observed in Muchalat when river outflow was high and an efflux when river outflow was lower.

Calculations of pCO_2 are also dependent on salinity, a parameter highly variable within the top 10m of the water column, on scales less than 1m (Figure 3). Measuring from a CTD can hide this small scale variability as measurements are taken at 1m depth intervals. Issues also arise from the setup of the rosette itself due to conductivity measurements being made ~0.5m metres below the bottom of each bottle, and bottles spanning a vertical distance of nearly 1m. When evaluating ΔpCO_2, particularly when gradients are small, potential error must also be considered and caution used when interpreting results. Table 2 summarises the air-sea pCO_2 gradient and calculated uncertainty. For 3 of the 13 stations the direction of the CO_2 flux changed within the range of the uncertainty.

Conclusion

In December 2015 outer Nootka Sound and Muchalat Inlet were shown to be a source of atmospheric CO_2, though values were often close to equilibrium and some stations appeared to act as a sink. The California Undercurrent was likely observed at a depth of 150-250m near the shelf break 60km offshore, however upwelling of these waters was not observed. High pCO_2 was observed in the deep basins of the fjord system, thought to be caused by respiration of organic matter. Nutrient data provided evidence for strong denitrification in the deep fjord waters, and also suggested an input of nutrients from open waters in outer Nootka Sound. The question of whether offshore water contributes to the high pCO_2 within deep basin water remains unanswered, and would require further study during the summer months when upwelling is favoured by the wind regime.

References

Borges, A. V. (2005). Do We Have Enough Pieces of the Jigsaw to Integrate CO2 Fluxes in the Coastal Ocean? *Estuaries*, *28*(1), 3–27. http://doi.org/10.1007/BF02732750

Carpenter, J. (1978). The Chesapeake Bay Institute Technique for the Winkler Dissolved Oxygen Method. http://www.aslo.org/lo/toc/vol_10/issue_1/0141.pdf

Castro, C. G., Chavez, F. P. and Collins, C. a. (2001). Role of the California undercurrent in the export of denitrified waters from the eastern tropical North Pacific. *Global Biogeochemical Cycles*, *15*(4), 819–830.

Chen, C. A. and Borges, A. (2009). Reconciling opposing views on carbon cycling in the coastal ocean: Continental shelves as sinks and near- shore ecosystems as sources of atmospheric CO2. *Deep Sea Research Part II: Topical Studies in Oceanography*, *56*, 578–590. http://doi.org/10.1016/j.dsr2.2008.12.009

Christensen, J. P. (1994). Carbon export from continental shelves, denitrification and atmospheric carbon dioxide. *Continental Shelf Research*, *14*(5), 547–576. http://doi.org/10.1016/0278-4343(94)90103-1

CO2SYS originally by Lewis and Wallace 1998, Converted to MATLAB by Denis Pierrot at CIMAS, University of Miami, Miami, Florida. Vectorization, internal refinements and speed improvements by Steven van Heuven, University of Groningen, The Netherlands. Accessed February 2016. http://cdiac.ornl.gov/ftp/co2sys/

Dickson, A. G., & Millero, F. J. (1987). A comparison of the equilibrium constants for the dissociation of carbonic acid in seawater media. *Deep Sea Research Part A, Oceanographic Research Papers*, *34*(10), 1733–1743. http://doi.org/10.1016/0198-0149(87)90021-5

Dickson, A. G. (1990). Standard potential of the reaction: AgCl(s) + 1/2H_2(g) = Ag(s) + HCl(aq), and the standard acidity constant of the ion HSO_4^- in synthetic sea water from 273.15 to 318.15 K. *The Journal of Chemical Thermodynamics*, *22*(2), 113–127. http://doi.org/10.1016/0021-9614(90)90074-Z

Dickson, G., Sabine, L. and Christian, R. (2007). *Guide to Best Practices for Ocean CO2 Measurements*. Sidney, Canada: North Pacific Marine Science Organization.

Dlugokencky, E. and Tans, P. (2015). *Global Monthly Mean CO2.*Available: http://www.esrl.noaa.gov/gmd/ccgg/trends/global.html. Last accessed 14th Nov 2015.

Fisheries and Oceans Canada. *Gold River 2015 Tide Tables.* Available: http://www.tides.gc.ca/eng/data/table/2015/wlev_sec/8650. Last accessed 10th May 2016.

Freeland, H.J., Denman, K.L., (1982). A topographically controlled upwelling center off southern Vancouver Island. *Journal of Marine Research*, 40, 1069–1093.

Gibbs Seawater Toolbox. Solubility of O2 in seawater version 3.05. Authors: Roberta Hamme, Paul Barker and Trevor McDougall (16th February, 2015).

Accessed: February 2016. http://www.teos-10.org/pubs/gsw/html/gsw_O2sol_SP_pt.html

Hedges, J. I., Baldock, J. a, Gelinas, Y., Lee, C., Peterson, M. L., & Wakeham, S. G. (2002). The biochemical and elemental compostions of marine plankton: A NMR prespective. *Mar. Chem.*, *78*, 47–63.

Hoppe, C. J. M., Langer, G., Rokitta, S. D., Wolf-Gladrow, D. a., & Rost, B. (2010). On CO_2 pertubation experiments: over-determination of carbonate chemistry reveals inconsistencies. *Biogeosciences Discussions*, *7*(2), 1707–1726. http://doi.org/10.5194/bgd-7-1707-2010

Huyer, a., Barth, J. a., Kosro, P. M., Shearman, R. K., & Smith, R. L. (1998). Upper-ocean water mass characteristics of the California current, Summer 1993. *Deep-Sea Research Part II: Topical Studies in Oceanography*, *45*, 1411–1442. http://doi.org/10.1016/S0967-0645(98)80002-7

Knox, C. (unpublished-2015) Are fjords sources or sinks of CO2? A study of air-sea CO2 fluxes in Nootka Sound, B.C. https://digital.lib.washington.edu/researchworks/handle/1773/33389

Koehlinger, J. (unpubished-2015) A Description of Water Masses in Nootka Sound and Estimation of Diffusivity (κ) and Upward Velocity (w) in Muchalat Inlet Using Temperature, Salinity, and Dissolved Oxygen. https://digital.lib.washington.edu/researchworks/handle/1773/33390

Lee, K., Kim, T. W., Byrne, R. H., Millero, F. J., Feely, R. A., and Liu, Y. M. (2010). The universal ratio of boron to chlorinity for the North Pacific and North Atlantic oceans. *Geochimica et Cosmochimica Acta*, *74*(6), 1801–1811. http://doi.org/10.1016/j.gca.2009.12.027

Lorenzen, C. (1967). Determination of chlorophyll and pheopigments: spectrophotometric equations. *Limnology and Oceanography*, *12*(1961), 343–346. http://doi.org/10.4319/lo.1967.12.2.0343

Murray, J., Roberts, E., Howard, E., O'Donnell, M., Bantam, C., Carrington, E., Foy, M., Paul, B. and Fay, A. (2015). An inland sea high nitrate-low chlorophyll (HNLC) region with naturally high pCO2. *Limnology and Oceanography,* 60, 957-966. http://doi.org/10.1002/lno.10062

NOAA. *Coastal Upwelling Indices.* Available: http://www.pfeg.noaa.gov/products/PFEL/modeled/indices/upwelling/NA/daily_upwell_graphs.html#p05daily.gif . Last accessed 10th May 2016.

No Author. (2013). *Environment Canada's Greenhouse Gas Measurements at Estevan Point.* Available: https://www.ec.gc.ca/mges-ghgm/default.asp?lang=En&n=F1A7FB1A-1. Last accessed April 2016.

Redfield, A C., Ketchum, B. H., and Richards, F. A. (1963). The influence of organisms on the composition of sea water. *The Sea*, (2), 26-77.

Sabine, C. L., Feely, R. A., Gruber, N., Key, R. M., Lee, K., Bullister, J. L., Wanninkhof, R., Wong, C., Wallace, D., Tilbrook, B., Millero, F., Peng, T., Kozyr, A., Ono, T. and Rios, A. F. (2004). The Oceanic Sink for Anthropogenic CO_2. *Nature*, *305*, 367–371. http://doi.org/10.1007/s13398-014-0173-7.2

Takahashi, T., Sutherland, S. C., Sweeney, C., Poisson, A., Metzl, N., Tilbrook, B., Bates, N., Wanninkhof, R., Feely, R., Sabine, C., Olafsson, J. and Nojiri, Y. (2002). Global sea-air CO2 flux based on climatological surface ocean pCO2, and seasonal biological and temperature effects. *Deep-Sea*

Research Part II: Topical Studies in Oceanography, *49*(9-10), 1601–1622. http://doi.org/10.1016/S0967-0645(02)00003-6

Thomson, R. E., & Krassovski, M. V. (2010). Poleward reach of the California Undercurrent extension. *Journal of Geophysical Research: Oceans*, *115*(9), 1–9. http://doi.org/10.1029/2010JC006280

Torres, R., Pantoja, S., Harada, N., González, H. E., Daneri, G., Frangopulos, M., Rutllant, J. A., Duarte, C. M., Ruiz-Halpern, S., Mayol, E. and Fukasawa, M. (2011). Air-sea CO_2 fluxes along the coast of Chile: From CO_2 outgassing in central northern upwelling waters to CO_2 uptake in southern Patagonian fjords. *Journal of Geophysical Research*, *116*(C9), C09006. http://doi.org/10.1029/2010JC006344

Tully, J. P. (1937). Oceanography of Nootka Sound. *Journal of the Biological Board of Canada*, *3*(1), 43–69. http://doi.org/10.1139/f37-005

Walsh, E., Ingalls, A. and Keil, R. (2008). Sources and transport of terrestrial organic matter in Vancouver Island fjords and the Vancouver-Washington Margin: A multiproxy approach using $\delta^{13}C_{org}$ lignin phenols, and the ether lipid BIT index. *Limnology and Oceanography*. 53 (3), 1054-1063. http://doi.org/10.4319/lo.2008.53.3.1054

Zeebe, R. and Wolf-Gladrow, D. (2001). Equilibrium. In: *CO2 in seawater: equilibrium, kinetics, isotopes*. Amsterdam: Elsevier. 1-37

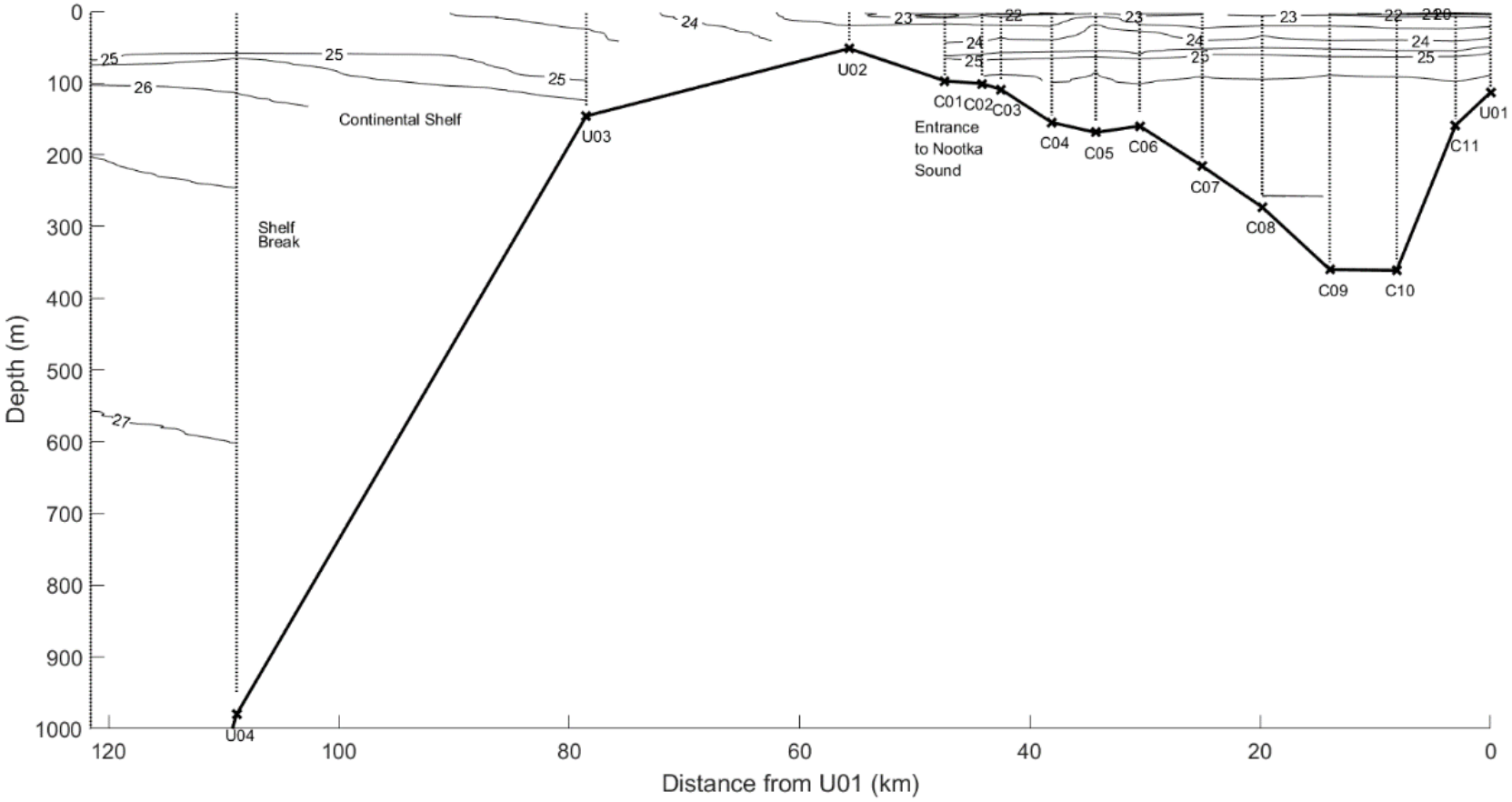

Figure 2 – Transect of density from the head of Muchalat Inlet (right) to 60km offshore. Black lines are isopycnals of 0.5kgm^{-3} (density-1000), thick black line represents each station depth with a line drawn between each station depth. Text indicates station names.

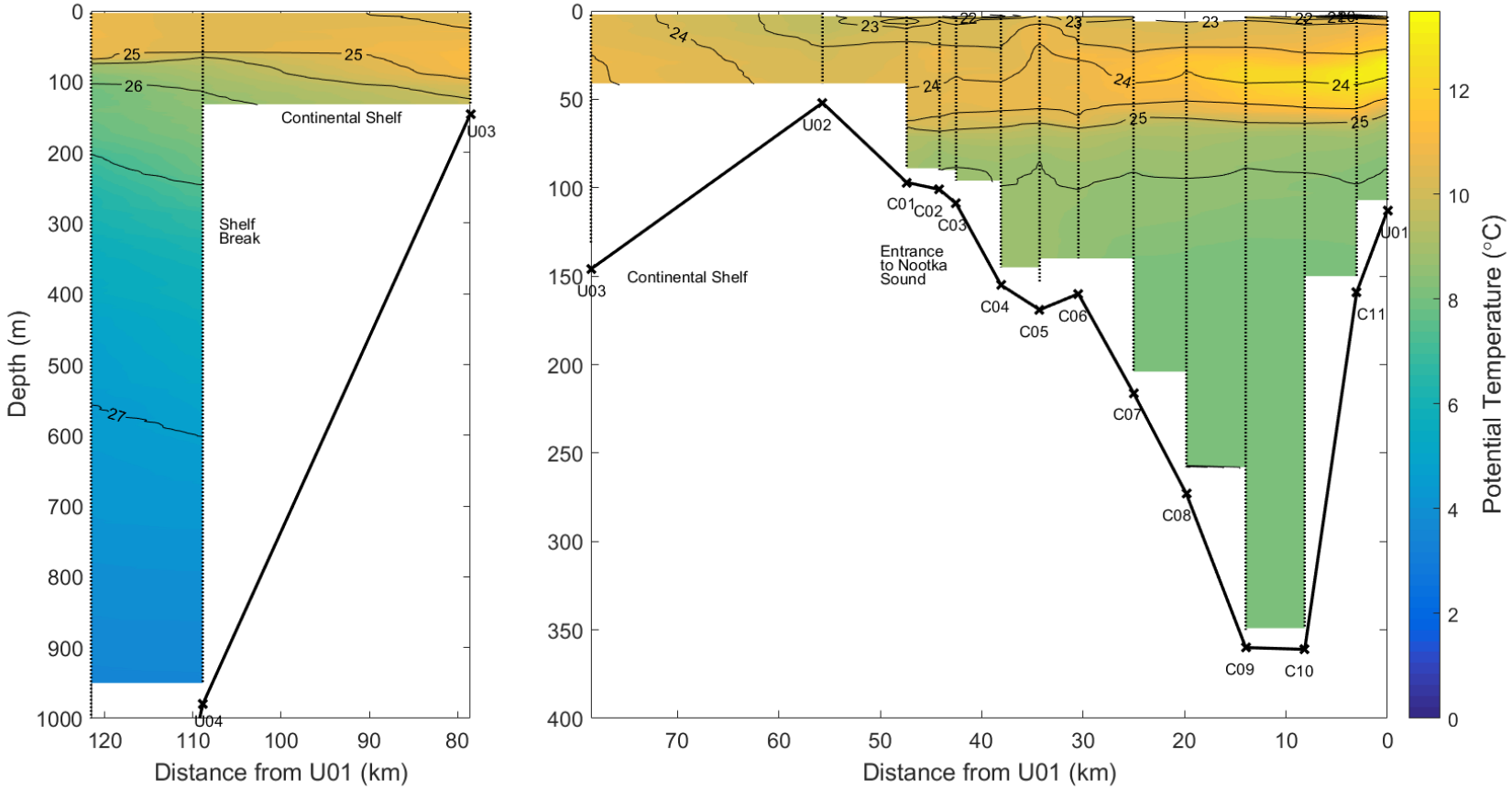

Figure 3 – Transect of potential temperature from the head of Muchalat Inlet (right) to 60km offshore. Black lines are isopycnals of 0.5kgm^{-3} (density-1000), dotted line marks locations of CTD casts, and thick black line represents each station depth with a line drawn between each station depth.

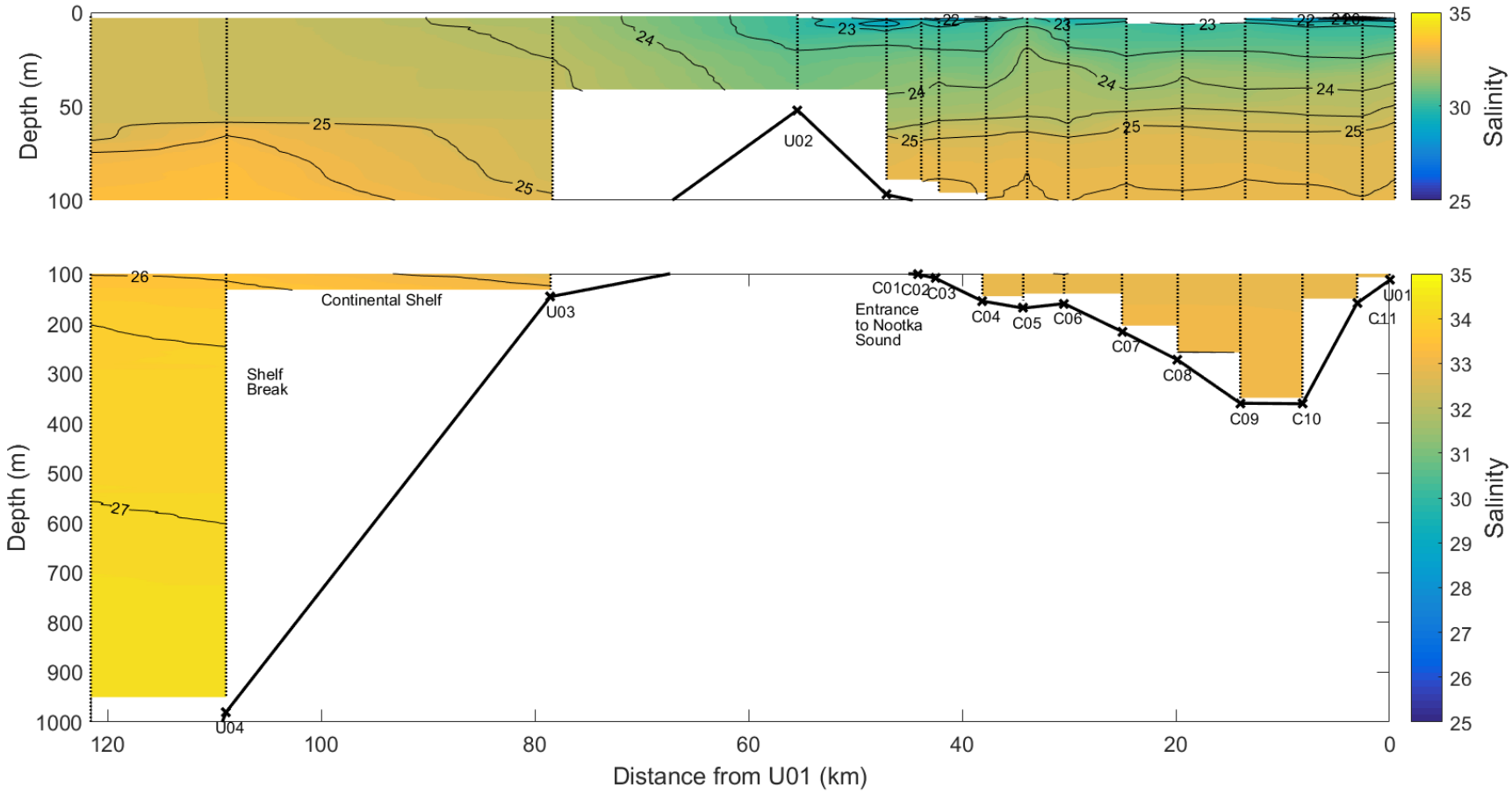

Figure 4 – Transect of salinity from the head of Muchalat Inlet (right) to 60km offshore to a depth of 100m. Black lines are isopycnals of 0.5kgm^{-3} (density-1000), dotted line marks locations of CTD casts.

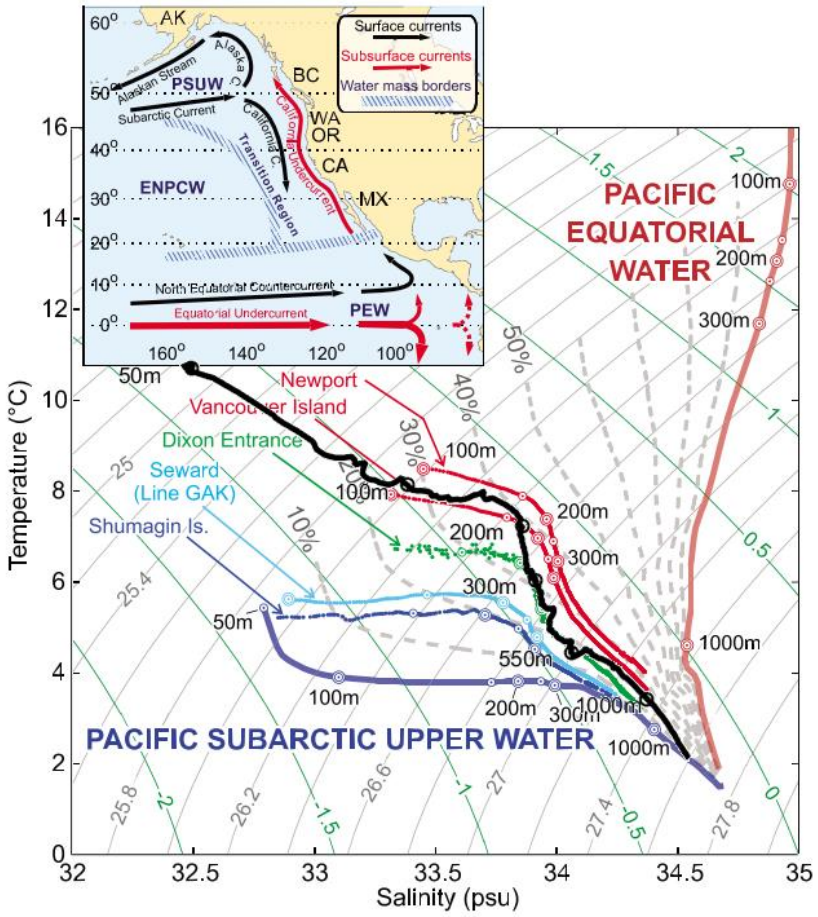

Figure 5 – Modified plot from Thomson and Krassovski (2010). Figure shows profiles of Pacific Equatorial Water (PEW) and Pacific Subarctic Water the two water masses thought to contribute to the California Undercurrent plotted in T-S space. Grey dotted lines indicate percentage of PEW. Black line is profile of 'Offshore' station from this study, depths are indicated by a larger black circle at 50m, 100m, 200m, 300m, 550m and 1000m.

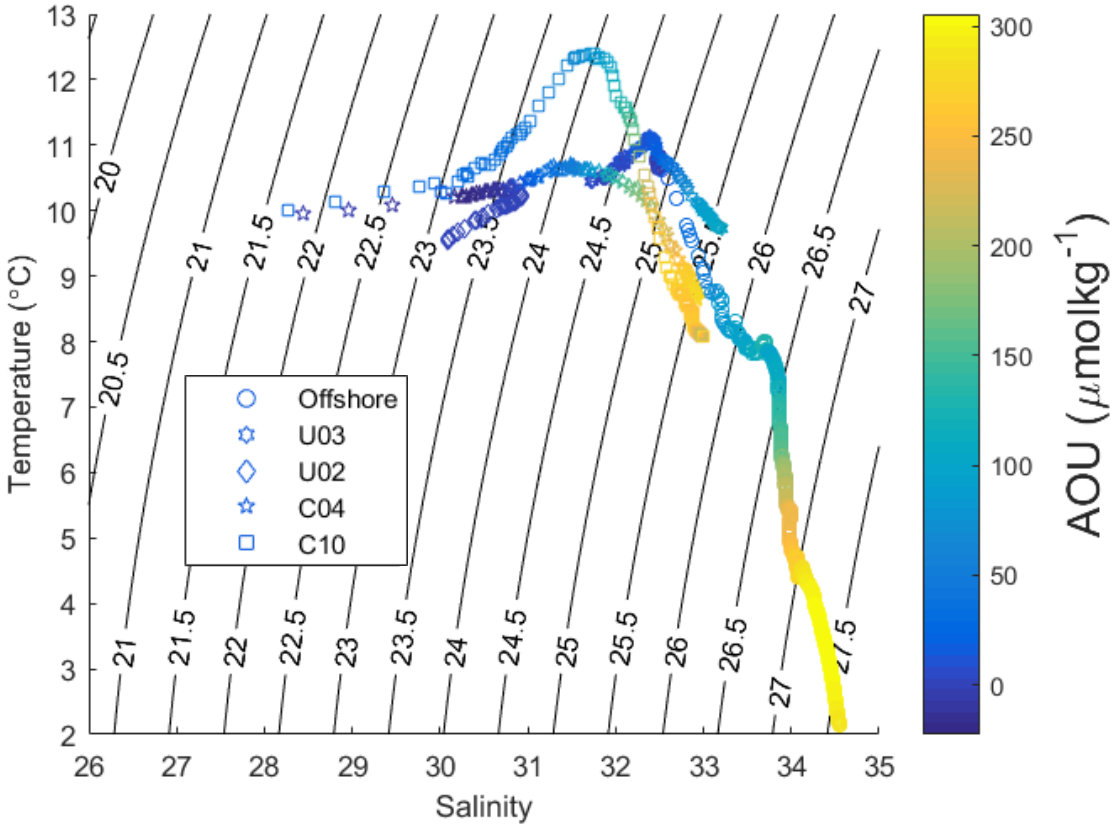

Figure 6- T-S diagram showing 5 depth profiles. C10 is within Muchalat Inlet, C04 is within Zuciarte Channel, U02 is over the outer sill, U03 is over the shelf and Offshore is just after the shelf break. Points are coloured according to apparent oxygen utilisation (AOU) at the corresponding depth.

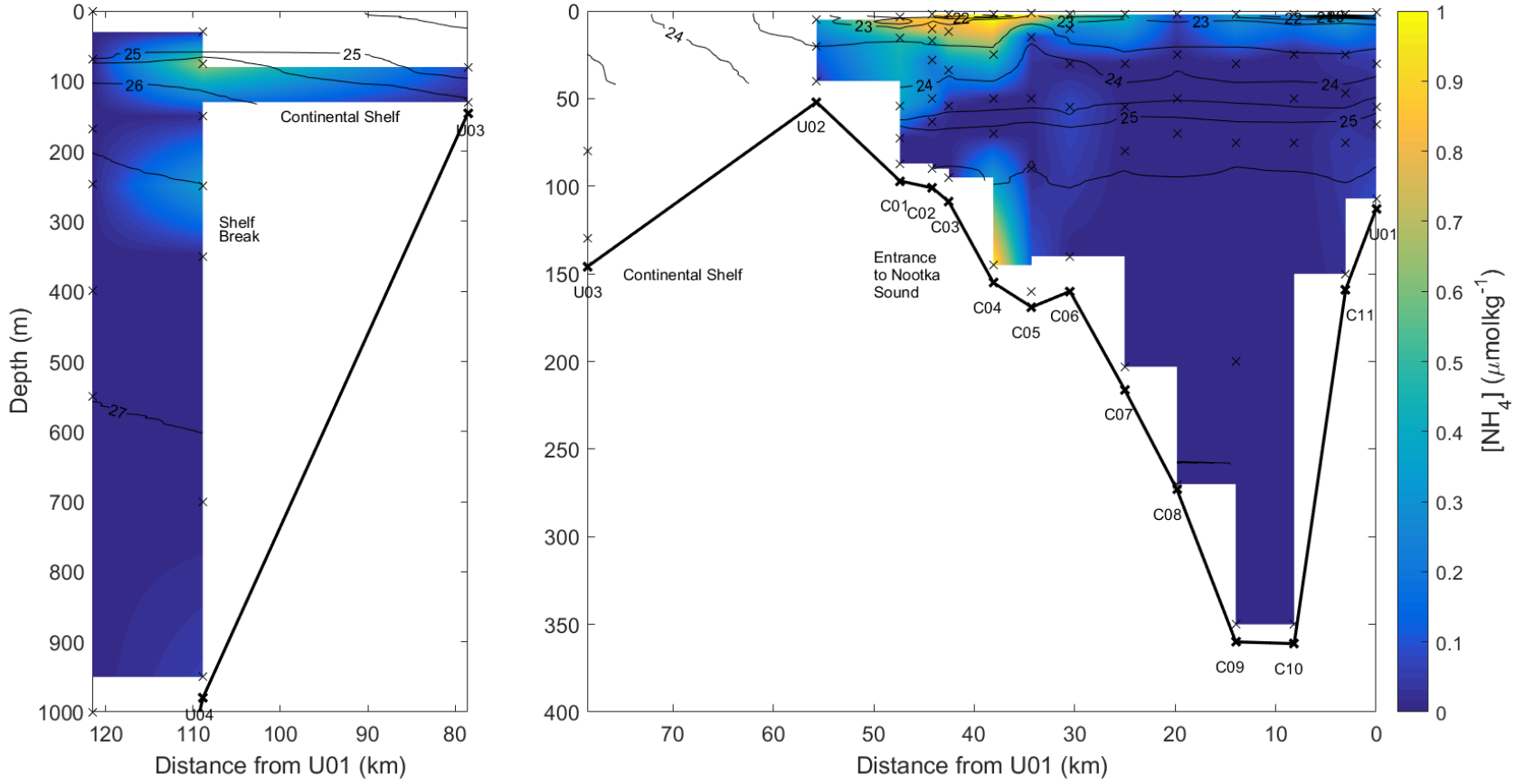

Figure 7 – Transect of ammonium concentrations from the head of Muchalat Inlet (right) to 60km offshore. Colour represents concentration, black lines are isopycnals of 0.5kgm^{-3} (density-1000), crosses mark locations where bottle data was taken, thick black line represents each station depth with a line drawn between each station depth.

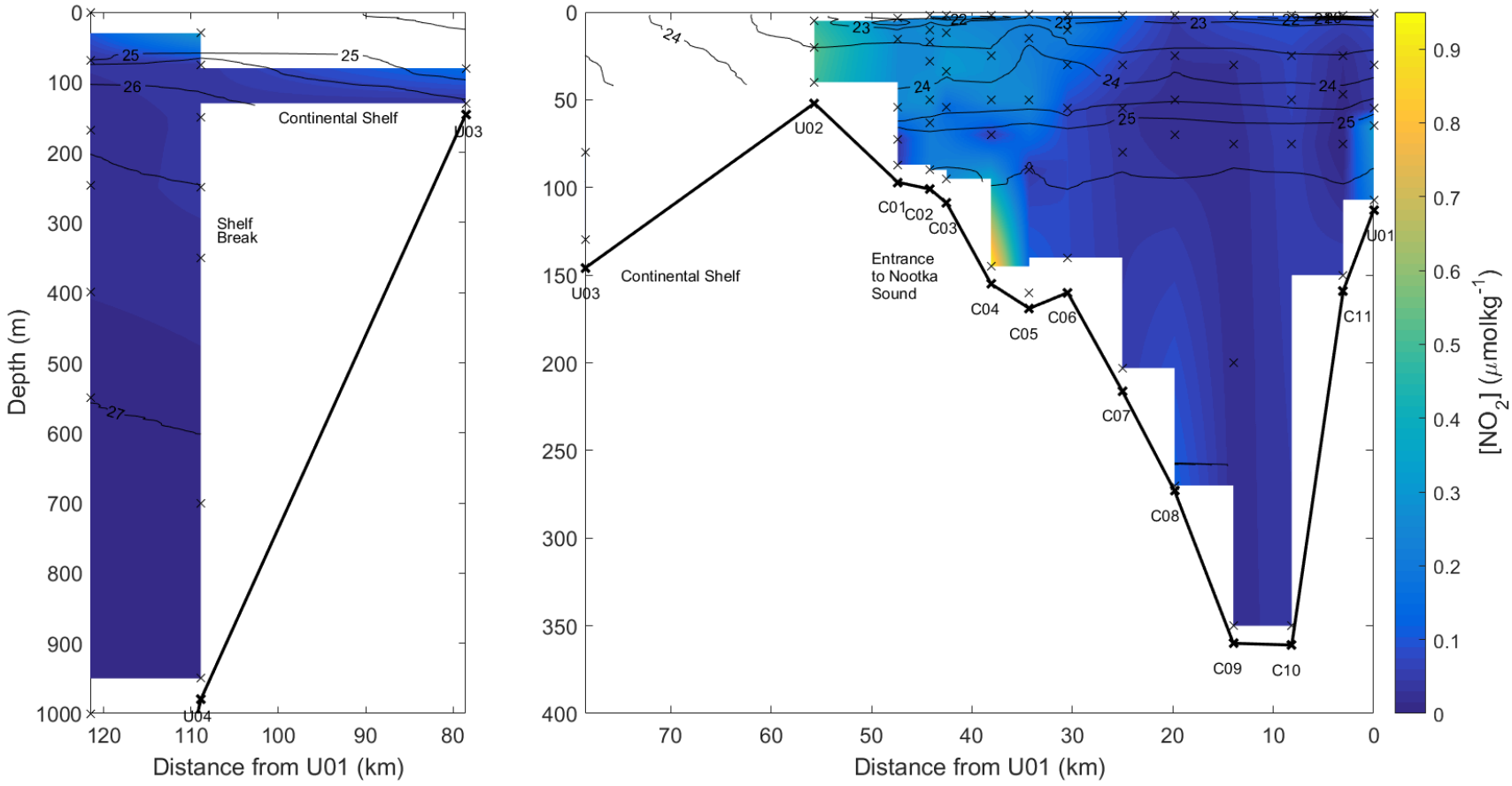

Figure 8 – Transect of nitrite concentrations from the head of Muchalat Inlet (right) to 60km offshore. Colour represents concentration, black lines are isopycnals of 0.5kgm^{-3} (density-1000), crosses mark locations where bottle data was taken, thick black line represents each station depth with a line drawn between each station depth.

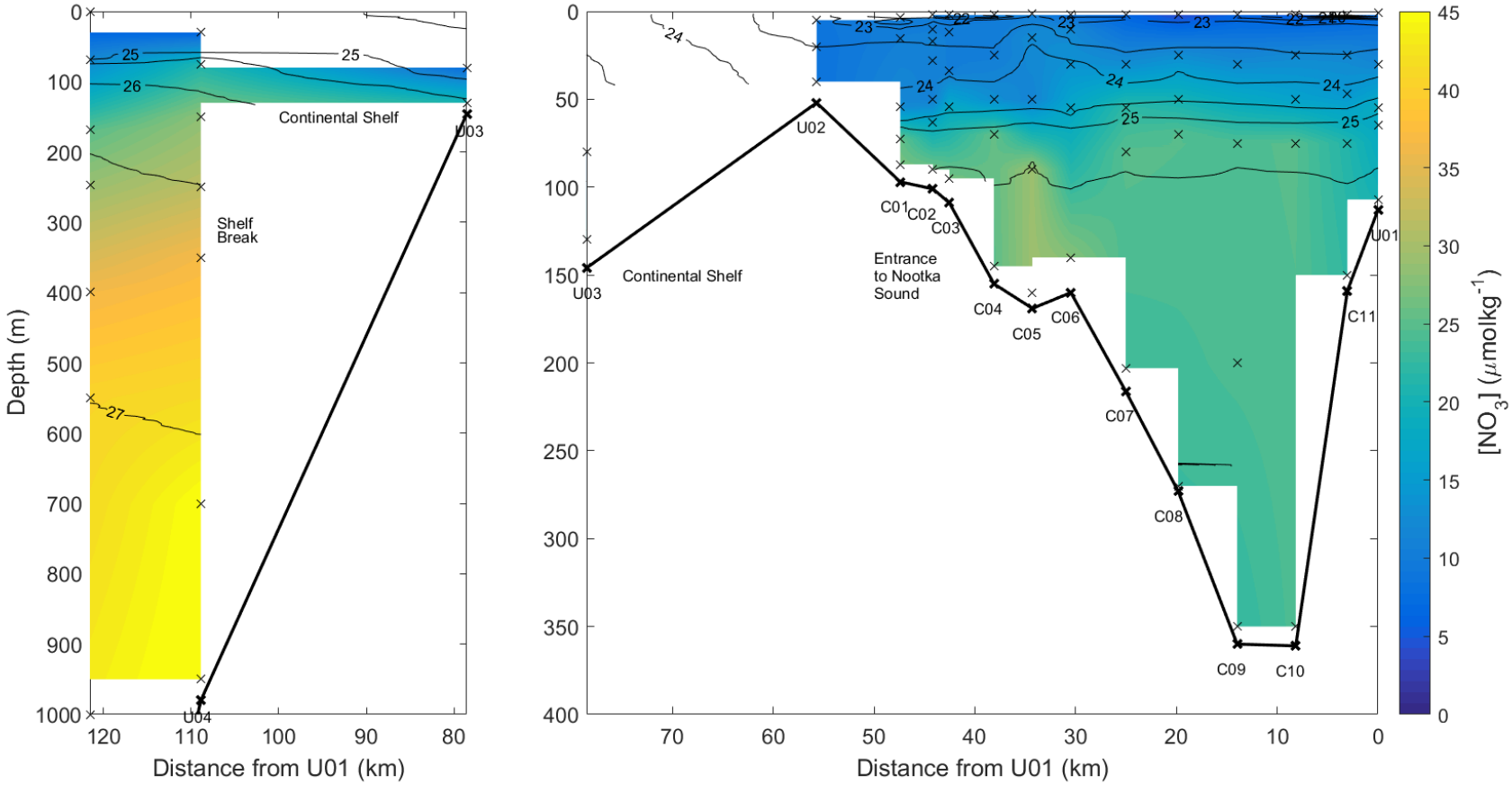

Figure 9– Transect of nitrate concentrations from the head of Muchalat Inlet (right) to 60km offshore. Colour represents concentration, black lines are isopycnals of 0.5kgm^{-3} (density-1000), crosses mark locations where bottle data was taken, thick black line represents each station depth with a line drawn between each station depth.

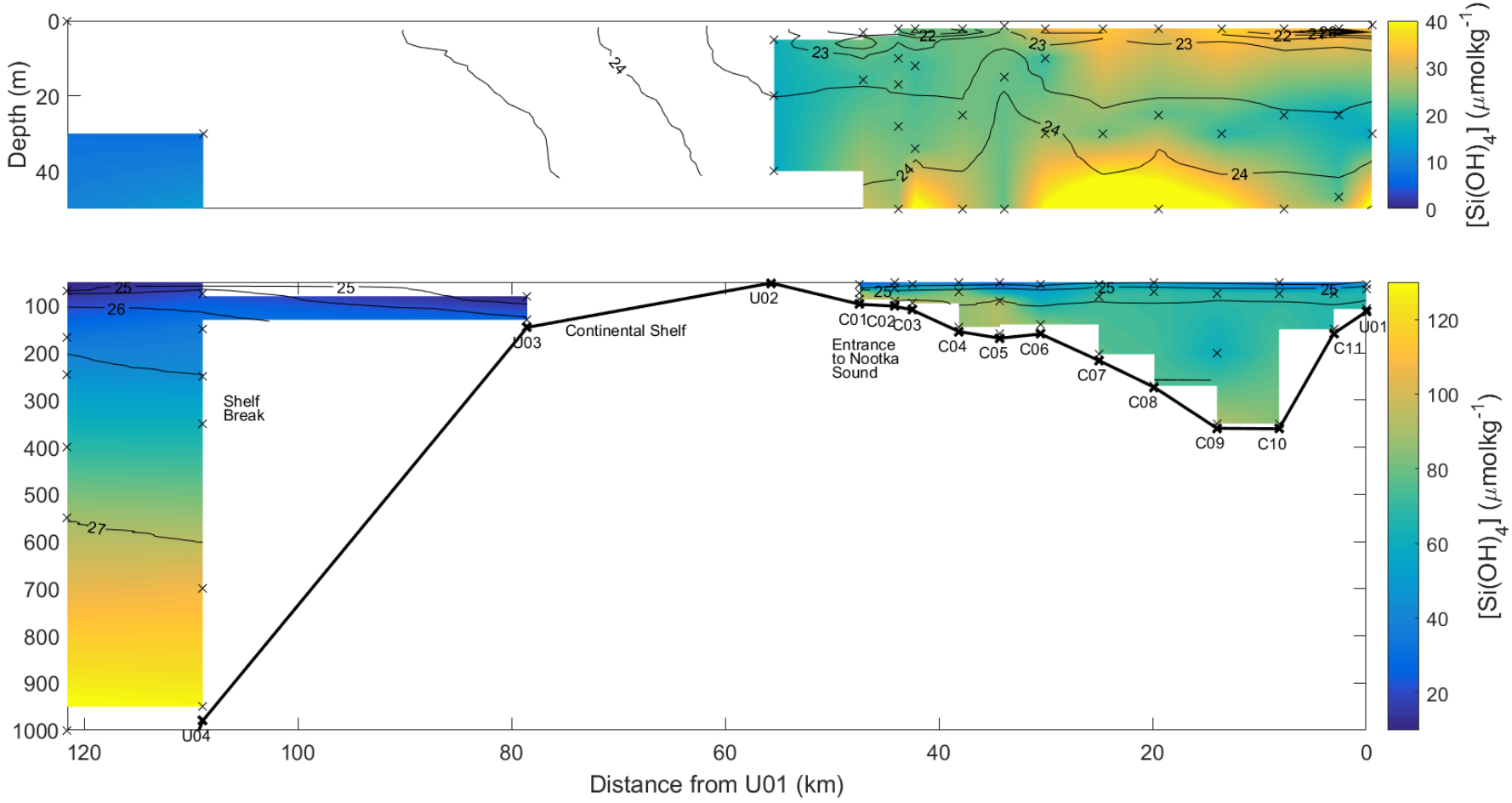

Figure 10 – Transect of silicate concentrations from the head of Muchalat Inlet (right) to 60km offshore. Colour represents concentration, black lines are isopycnals of 0.5kgm^{-3} (density-1000), crosses mark locations where bottle data was taken, thick black line represents each station depth with a line drawn between each station depth. Note different colour scale.

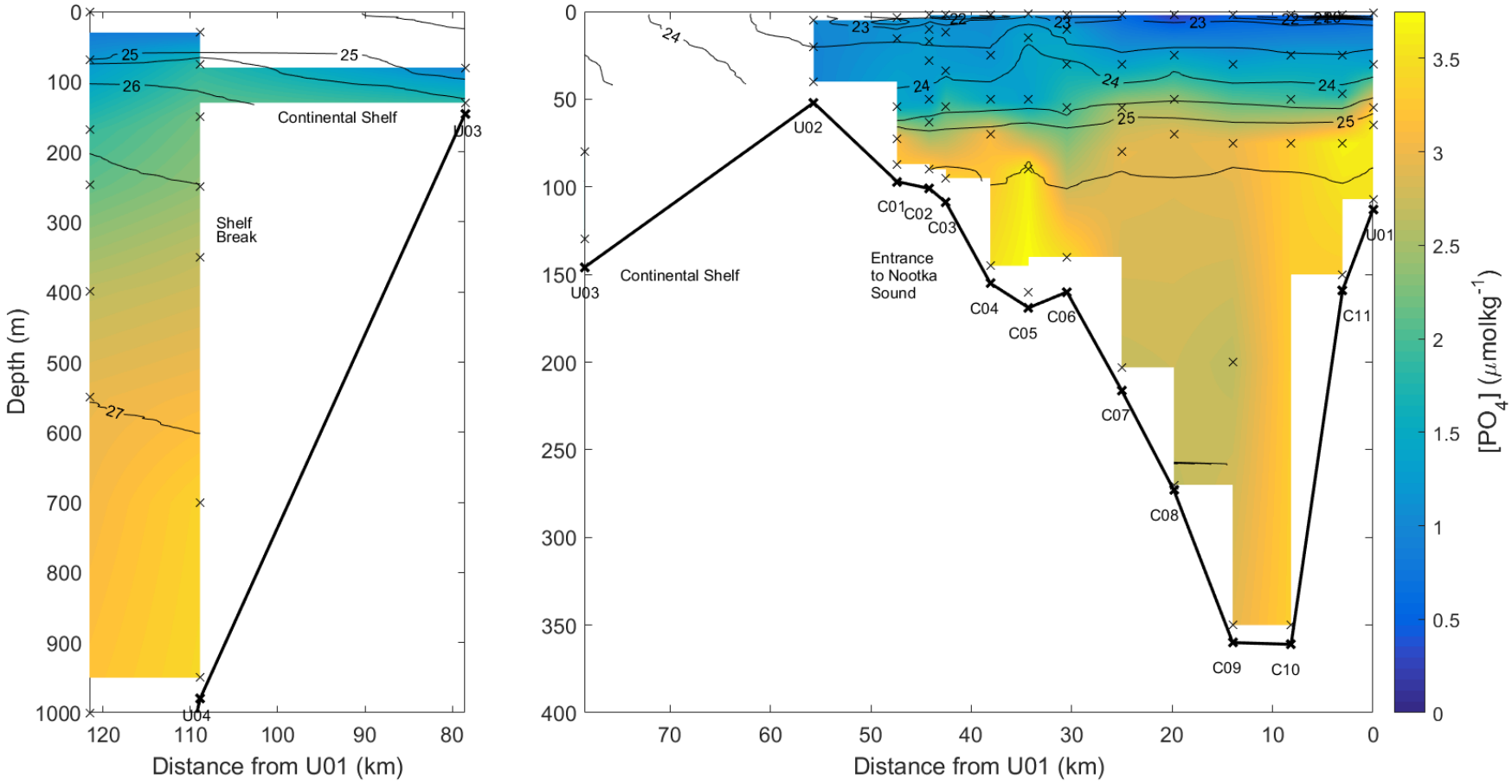

Figure 11 – Transect of phosphate concentrations from the head of Muchalat Inlet (right) to 60km offshore. Colour represents concentration, black lines are isopycnals of 0.5kgm^{-3} (density-1000), crosses mark locations where bottle data was taken, thick black line represents each station depth with a line drawn between each station depth.

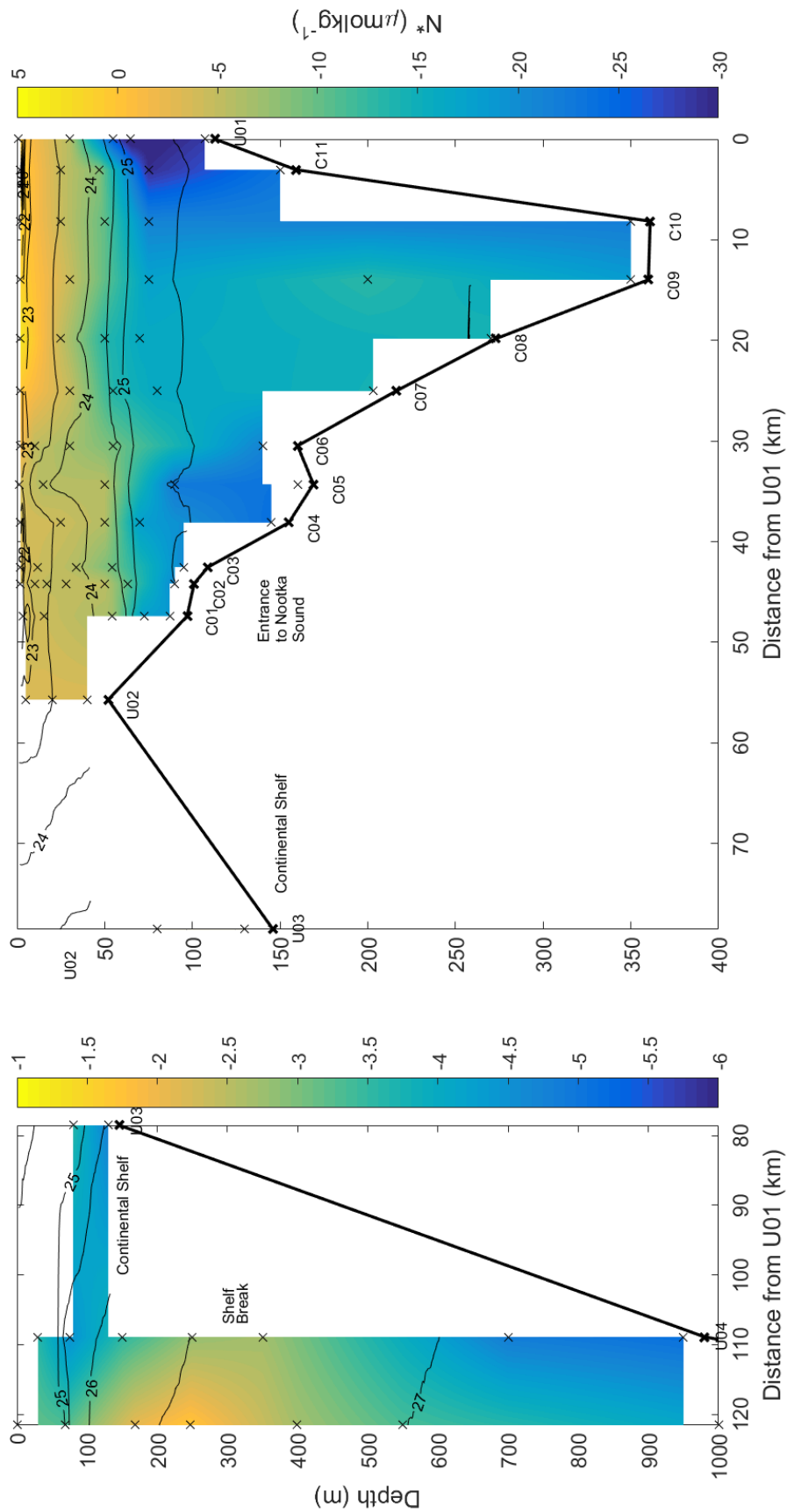

Figure 12 – Transect of N* from the head of Muchalat Inlet (right) to 60km offshore. Black lines are isopycnals of 0.5kgm^{-3} (density-1000), dotted line marks locations of CTD casts, and thick black line represents each station depth with a line drawn between each station depth. Transect separated to show, variation at lower N* values offshore, gradient of colour is on a different scale for each section.

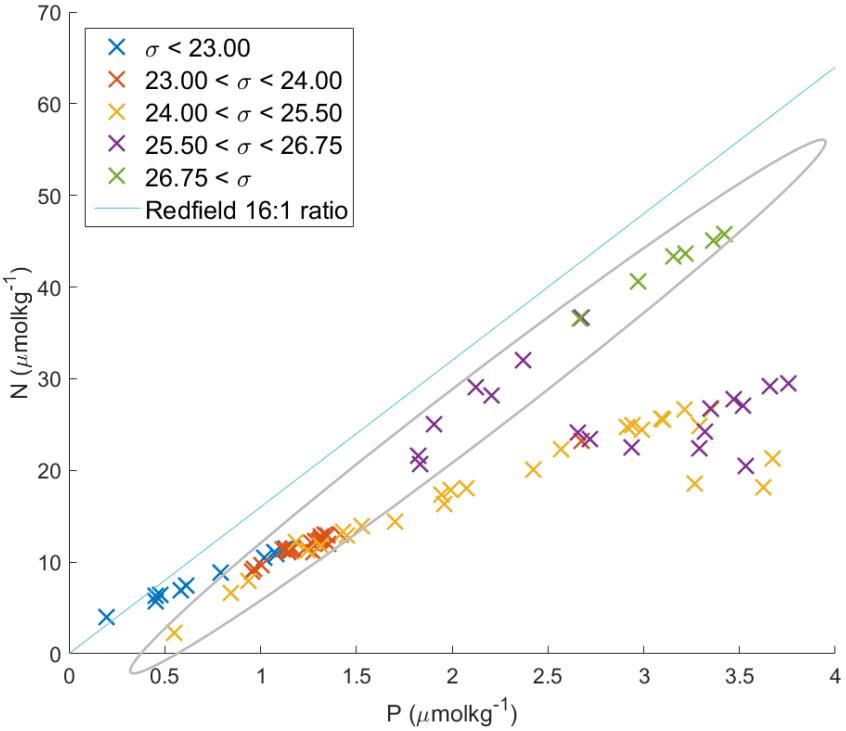

Figure 13 - Plot showing relationship between nitrogen (nitrate + nitrite + ammonium) and phosphate concentration. Data points are from all stations from within Muchalat Inlet to Offshore and are colour-coded as in figure 13. Blue line indicates theoretical relation described by Redfield (Redfield *et al*,. 1963). Grey circle indicates offshore data points .Error-bars are not shown on plot as they are not visible on this scale, for reference error in N is ±0.19µmolkg^{-1}, error in P is 0.03µmolkg^{-1}.

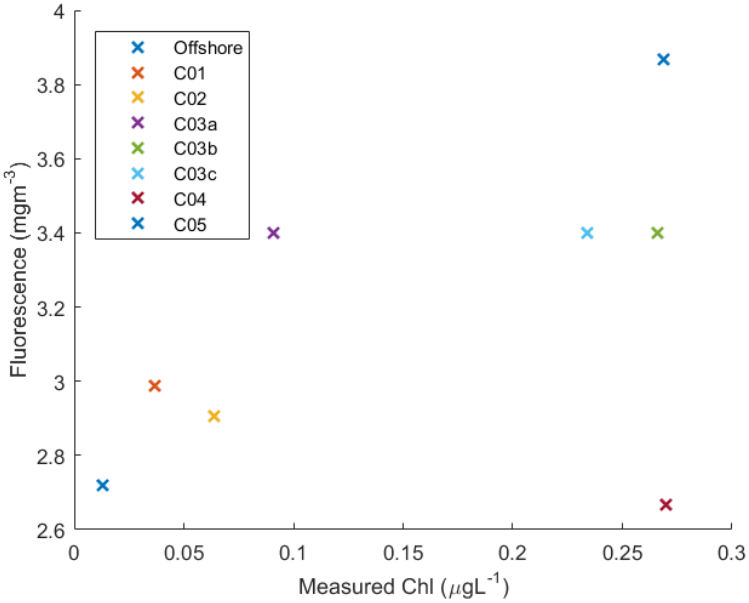

Figure 14- Plot to show correlation between measured chlorophyll data and fluorescence values obtained using the fluorometer on the CTD rosette. Each point represents a different station with a triplicate taken at station C03.

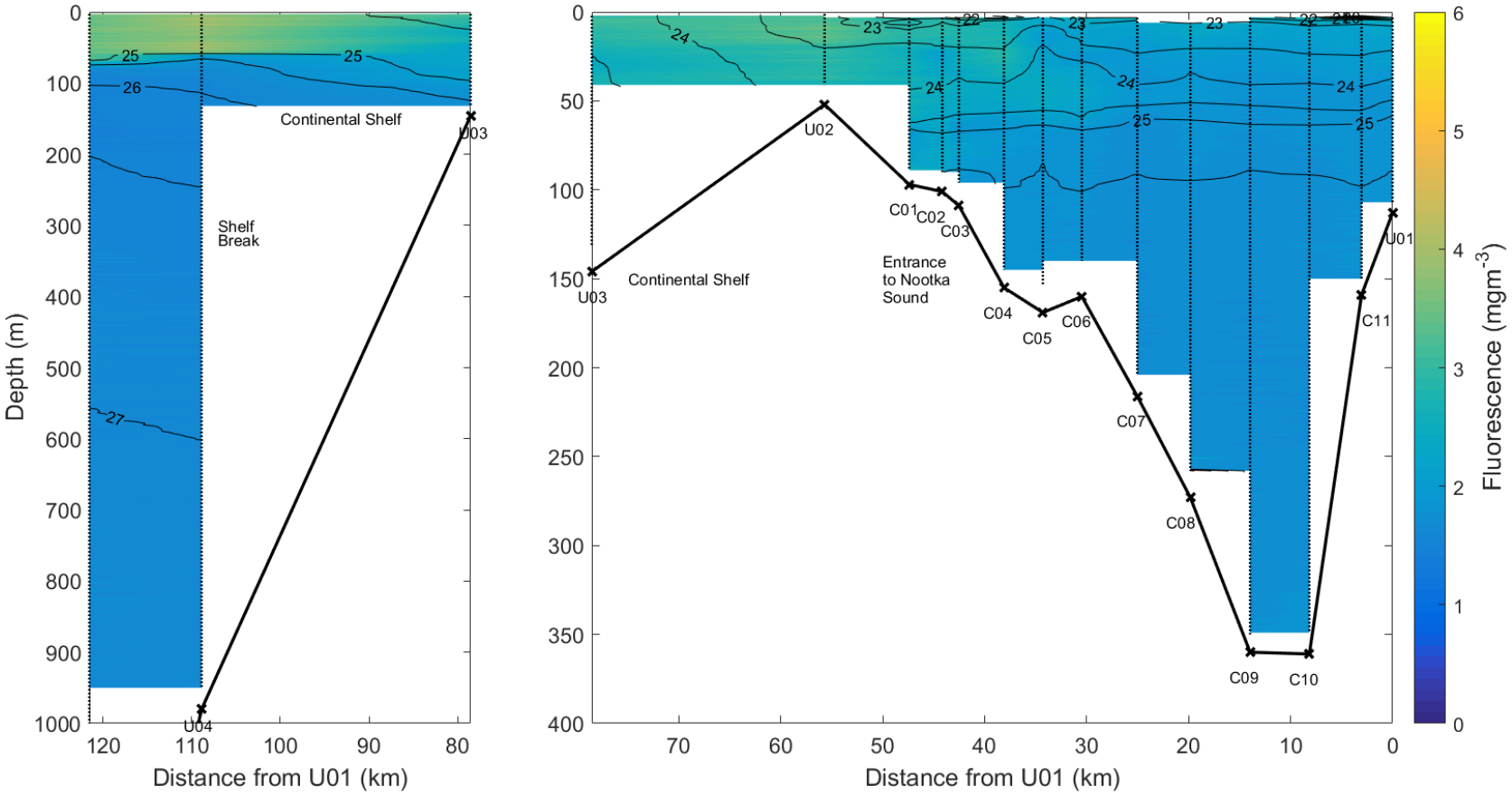

Figure 15 – Transect of Fluorescence from the head of Muchalat Inlet (right) to 60km offshore. Black lines are isopycnals of 0.5kgm^{-3} (density-1000), dotted line marks locations of CTD casts, and thick black line represents each station depth with a line drawn between each station depth.

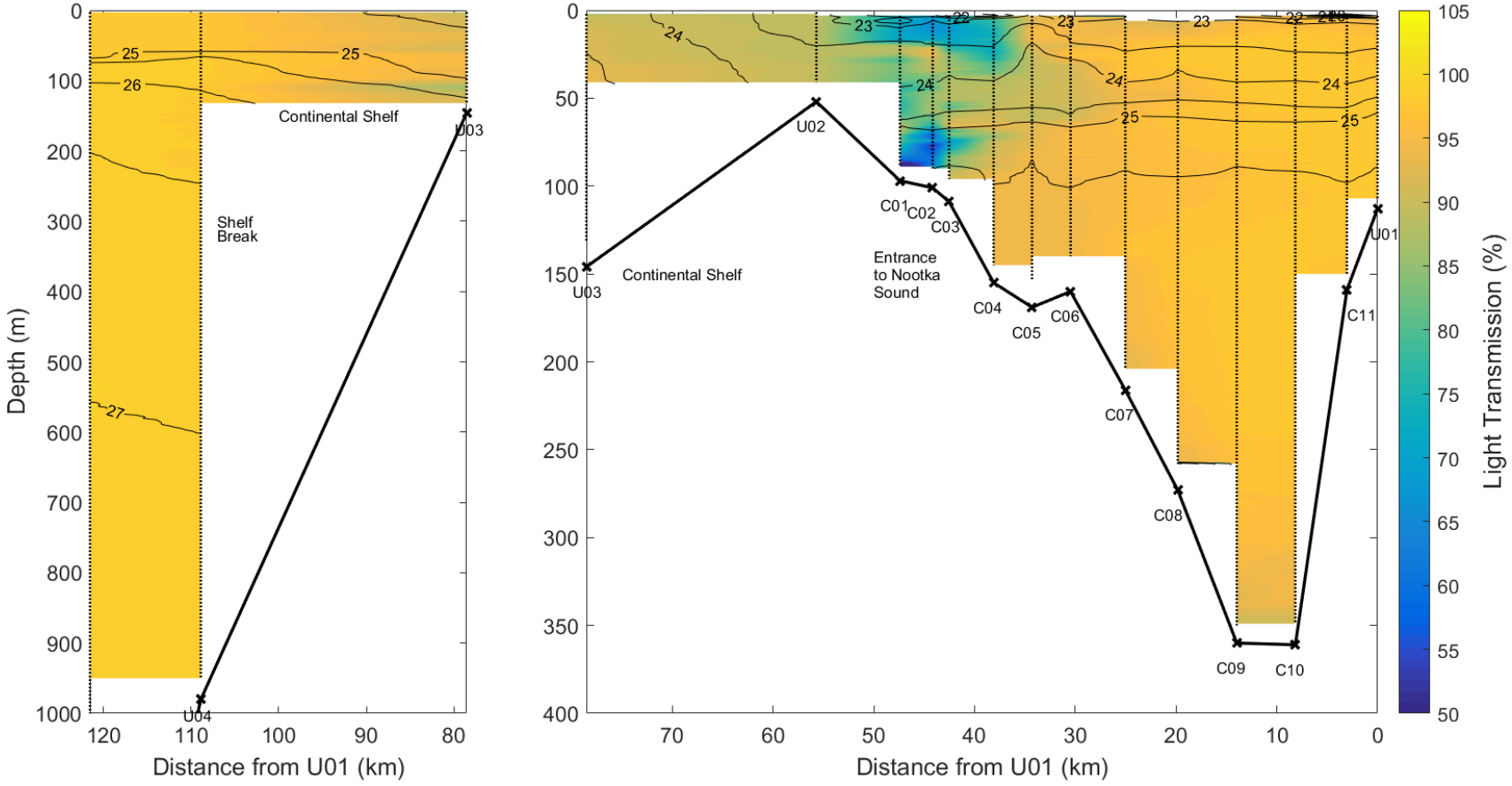

Figure 16 – Transect of turbidity from the head of Muchalat Inlet (right) to 60km offshore. Colour represents concentration, black lines are isopycnals of 0.5kgm^{-3} (density-1000), dotted line marks locations of CTD casts, and thick black line represents each station depth with a line drawn between each station depth.

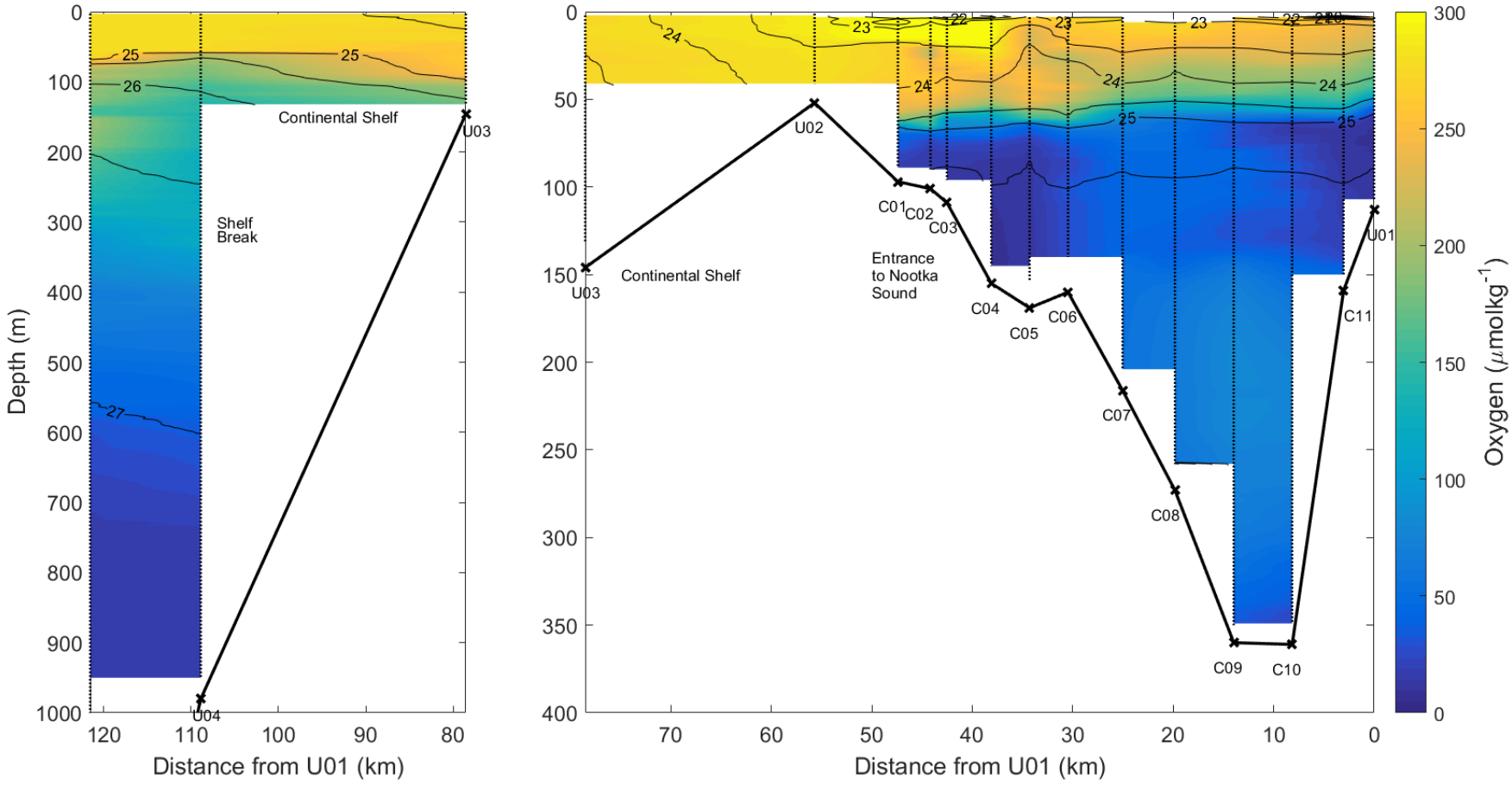

Figure 17 – Transect of oxygen concentrations (using optode data) from the head of Muchalat Inlet (right) to 60km offshore. Colour represents concentration, black lines are isopycnals of 0.5kgm^{-3} (density-1000), vertical dotted line marks CTD cast where data was obtained, thick black line represents each station depth with a line drawn between each station depth.

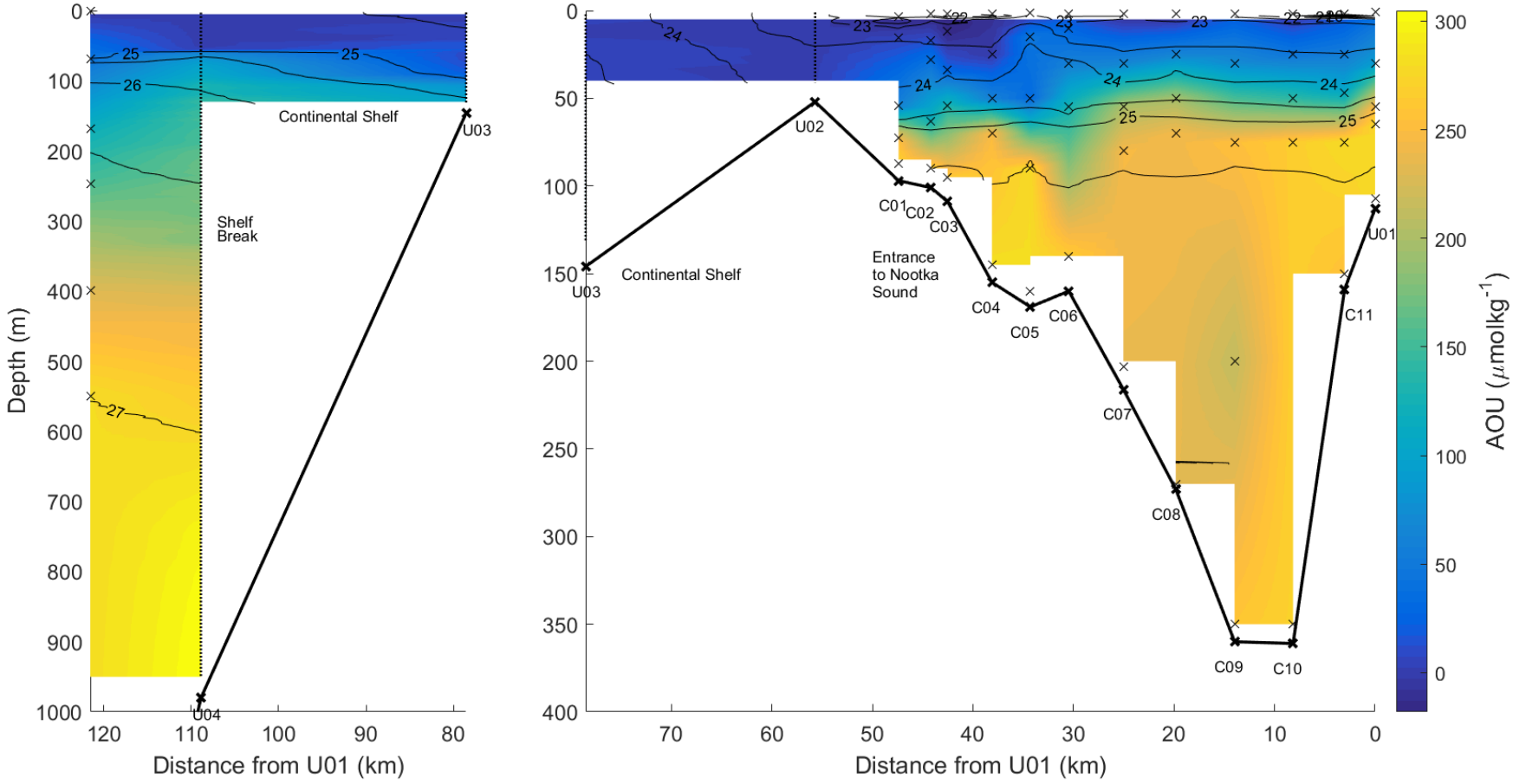

Figure 18 – Transect of apparent oxygen utilisation (AOU) from the head of Muchalat Inlet (right) to 60km offshore. Colour represents concentration, black lines are isopycnals of 0.5kgm^{-3} (density-1000), crosses mark locations where bottle data was taken, vertical dotted lines indicate stations where CTD optode data was used in the absence of bottle samples, thick black line represents each station depth with a line drawn between each station depth.

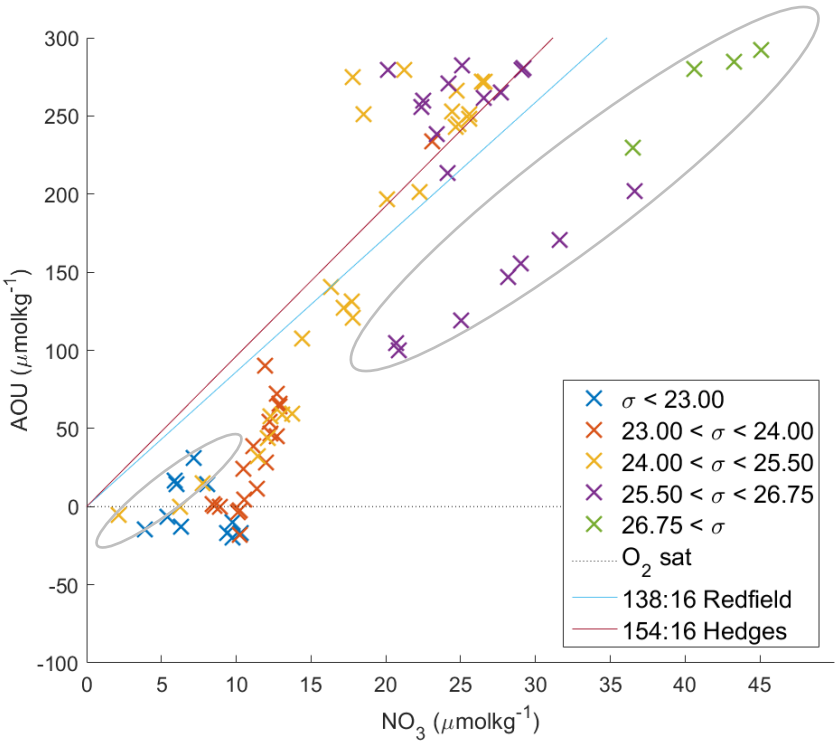

Figure 19 - Plot showing relationship between apparent oxygen utilisation (AOU) and nitrate concentration. Data points are from all stations from within Muchalat Inlet to offshore and are colour-coded according to density as described in the figure legend. Within the fjord system blue generally corresponds to upper 10m of water column, orange to upper 50m, remaining density intervals are arbitrary with purple corresponding to densities expected of the California Undercurrent. Dotted line indicates oxygen saturation, blue and red lines indicate gradients of theoretical relationship described by Redfield (Redfield *et al*., 1963) and Hedges (Hedges *et al*., 2002) respectively. Grey circle indicates offshore data points. 1 standard deviation in AOU is ±6.8µmolkg^{-1} , minimum detection limit of NO_3 is ±0.15µmolkg^{-1}.

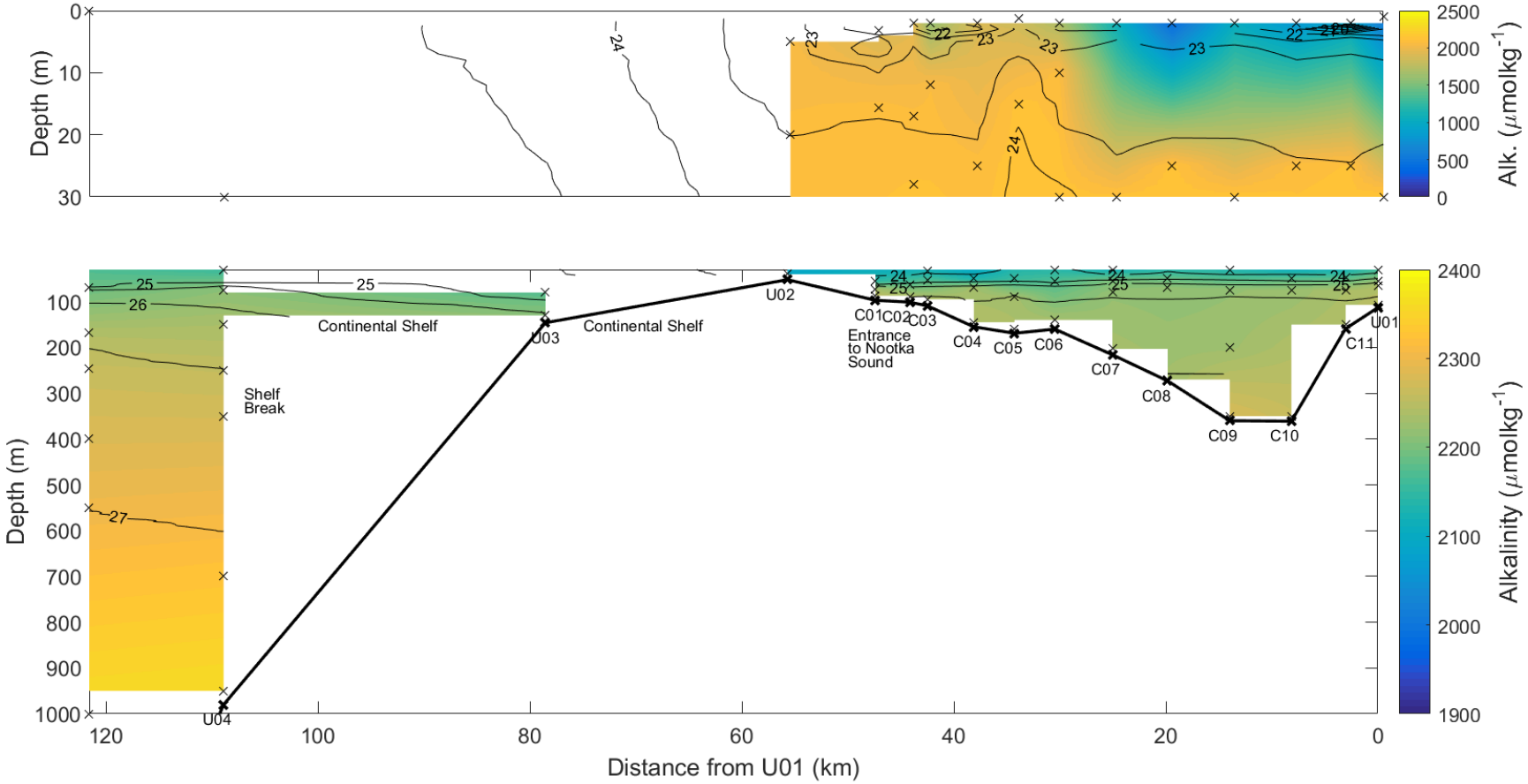

Figure 20 – Transect of alkalinity (alk) from the head of Muchalat Inlet (right) to 60km offshore. Colour represents concentration, black lines are isopycnals of 0.5kgm^{-3} (density-1000), crosses mark locations where bottle data was taken, and thick black line represents each station depth with a line drawn between each station depth. Plot is split to show upper 30m in detail on a different colour scale, bottom plot is from 30m-950m.

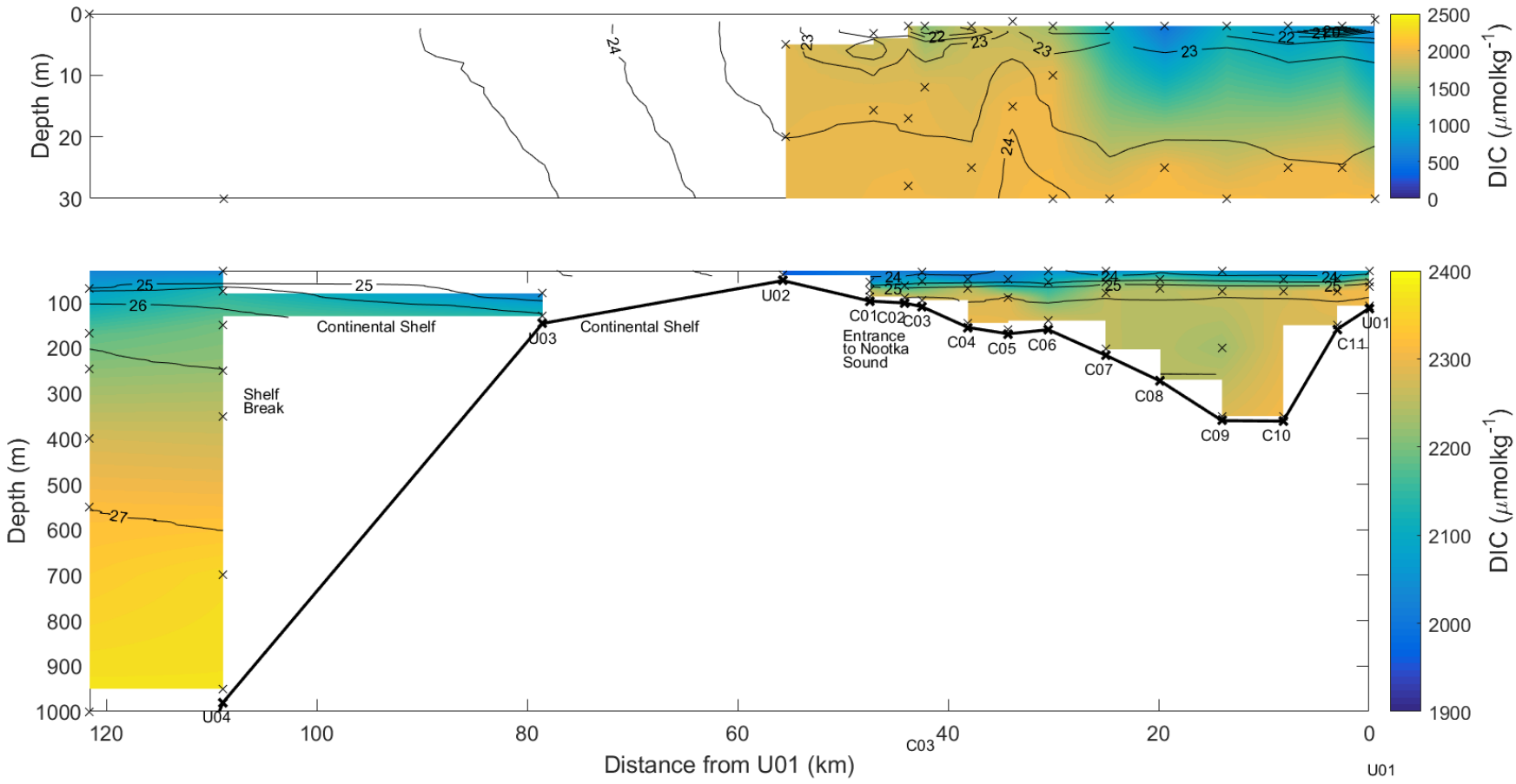

Figure 21 – Transect of dissolved inorganic carbon (DIC) concentrations from the head of Muchalat Inlet (right) to 60km offshore. Colour represents concentration, black lines are isopycnals of 0.5kgm^{-3} (density-1000), crosses mark locations where bottle data was taken, and thick black line represents each station depth with a line drawn between each station depth. Plot is split to show upper 30m in detail on a different colour scale, bottom plot is from 30m-950m.

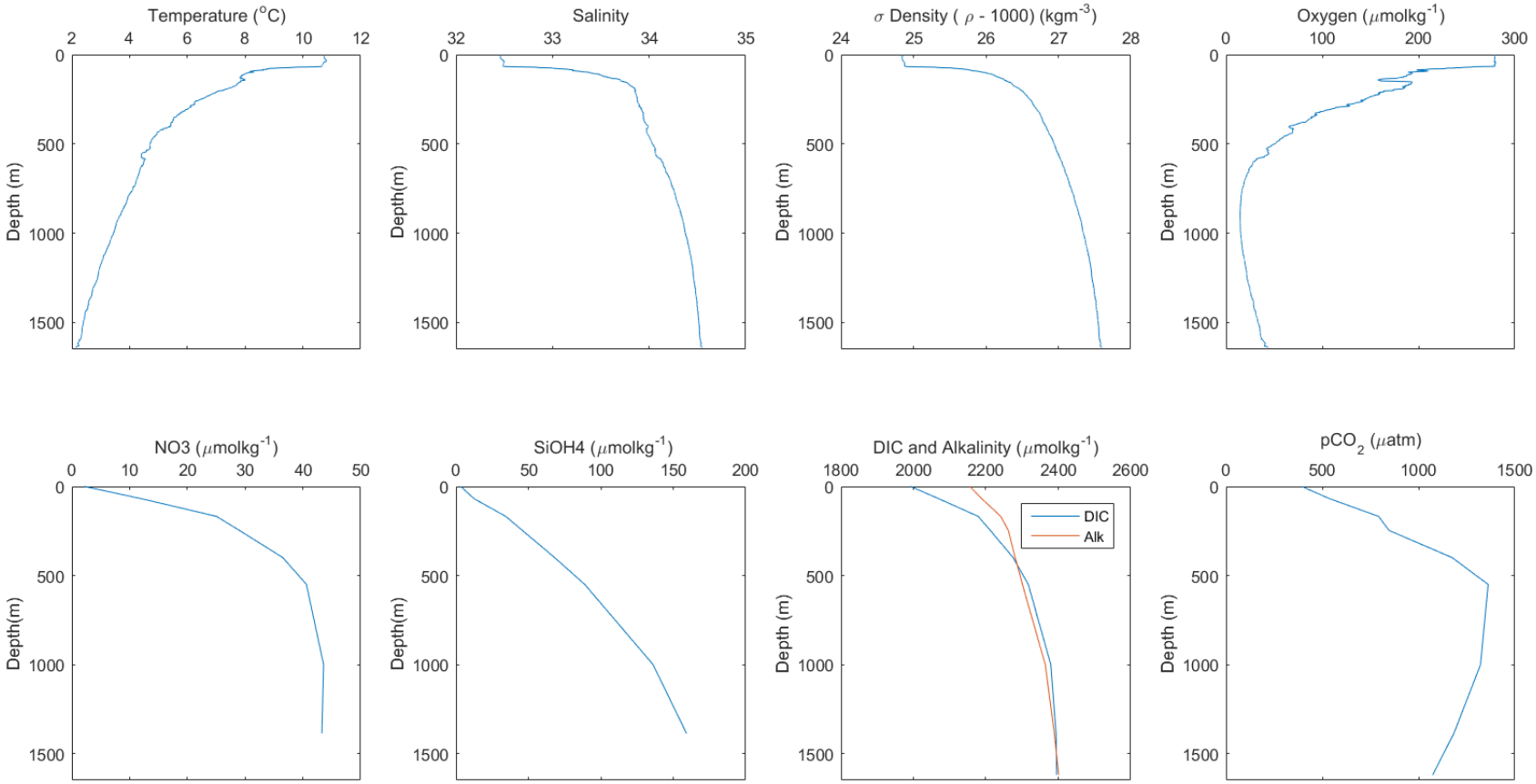

Figure 22 – Vertical profiles (from left to right) of (top) temperature, salinity, density, oxygen, (bottom) nitrate, silicate , DIC and alkalinity, pCO_2 at the Offshore station. Parameters on top row use data from the CTD profile, bottom row uses bottle data taken from a separate cast on a different day (see Table 1).

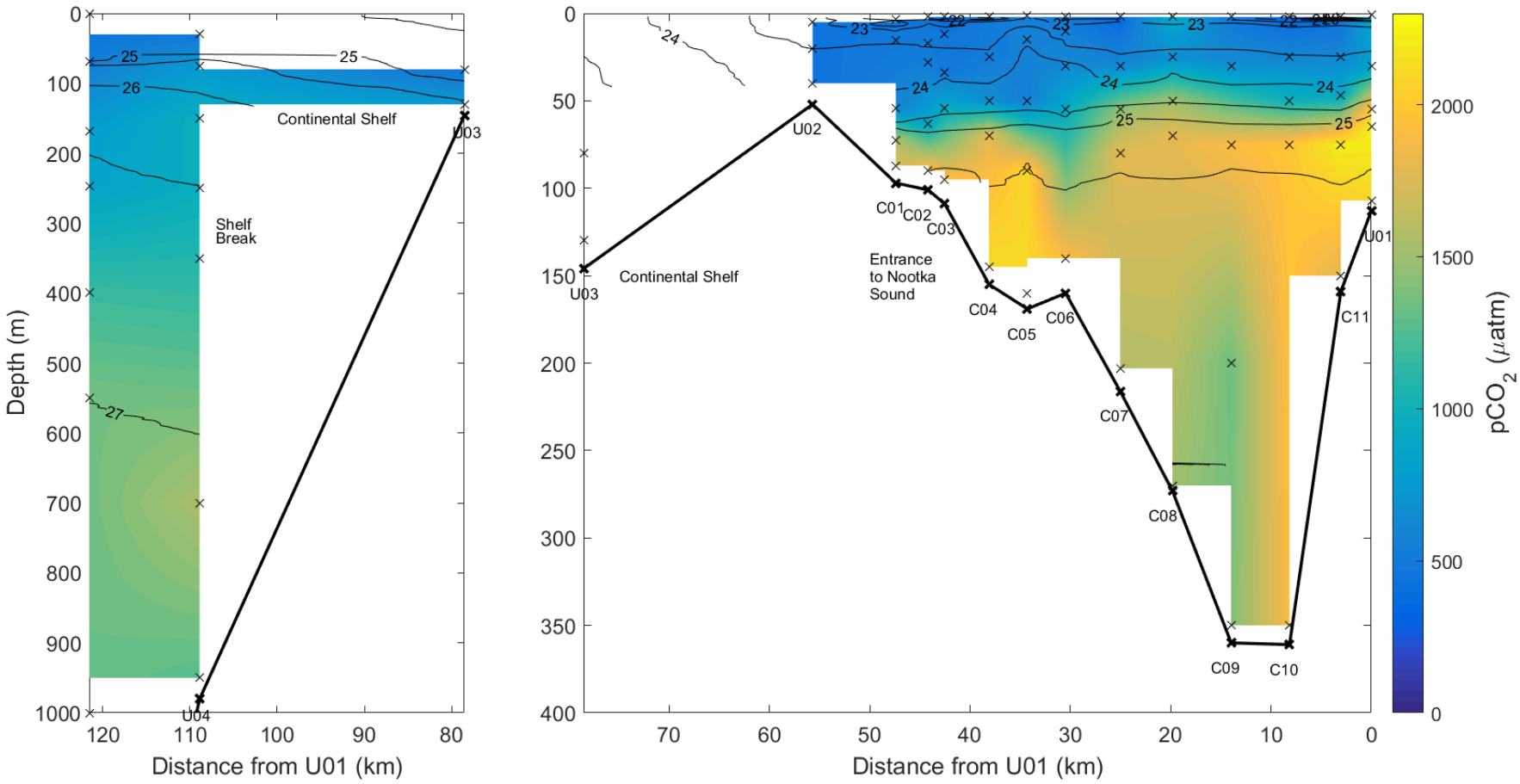

Figure 23 – Transect of pCO_2 concentrations from the head of Muchalat Inlet (right) to 60km offshore. Colour represents concentration, black lines are isopycnals of 0.5kgm^{-3} (density-1000), crosses mark locations where bottle data was taken, and thick black line represents each station depth with a line drawn between each station depth.

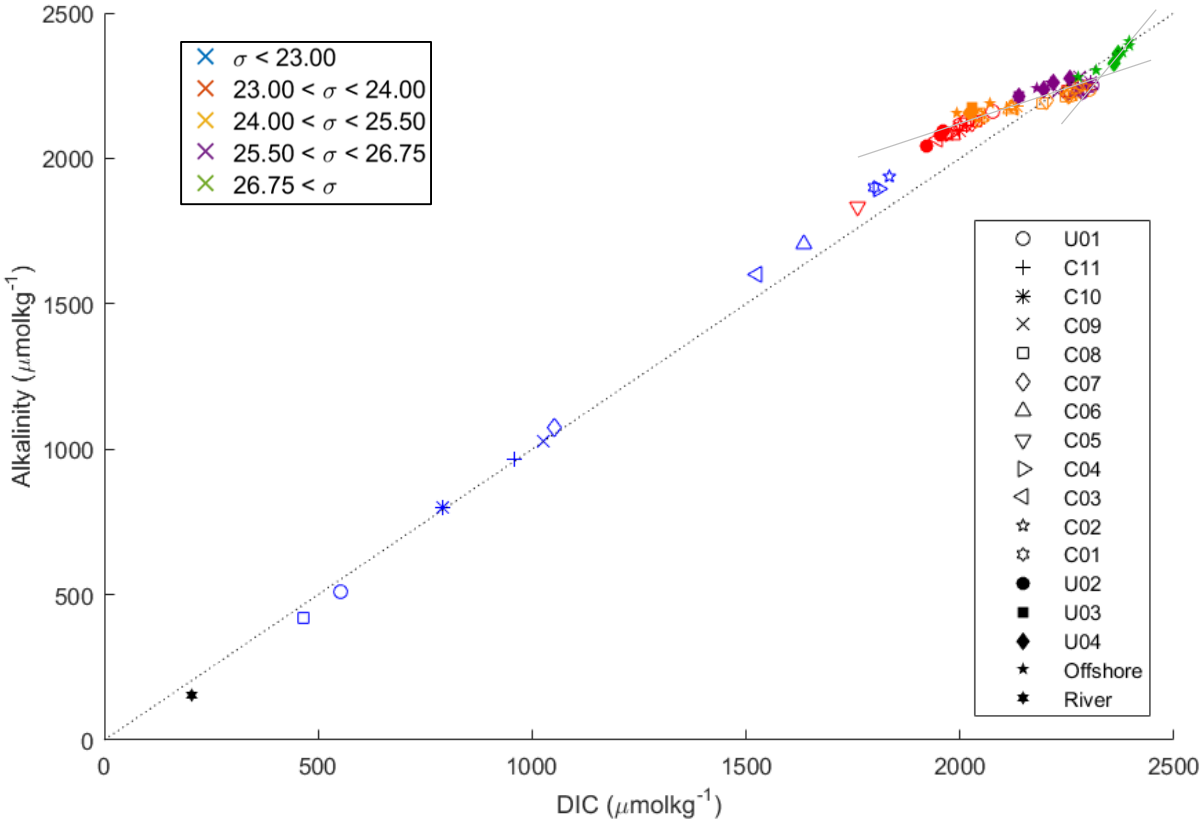

Figure 24 - Plot showing relationship between alkalinity and DIC concentration. Data points are from all stations from within Muchalat Inlet to Offshore and are colour-coded according to density as described in figure 13. Shapes as shown by the legend indicate station at which data was taken. Grey solid lines highlight areas of differing gradient (not fitted), dotted grey line indicates a gradient of 1. Error bars are not included, as conservative errors of 5µmolkg^{-1} (1 std. dev.) for both alkalinity and DIC cannot be seen on this scale.

Date (DD/MM/YYYY)	1st High Tide		2nd High Tide		1st Low Tide		2nd Low Tide	
	Time (GMT)	Height (m)	Time (GMT)	Height (m)	Time (GMT)	Height (m)	Time (GMT)	Height (m)
12/12/2015	04:31	3.8	18:01	3.4	11:24	0.4	23:24	0.4
13/12/2015	05:10	3.8	16:41	3.4	12:02	0.5	-	-
14/12/2015	05:53	3.7	19:24	3.4	00:08	1.8	12:42	0.5
16/12/2015	07:33	3.4	20:59	3.5	01:53	1.8	14:12	0.8
19/12/2015	11:15	2.9	23:44	3.7	05:23	1.4	17:06	1.4

Table 4- Tide time and tidal height at Gold River during period of study (www.tides.gc.ca).

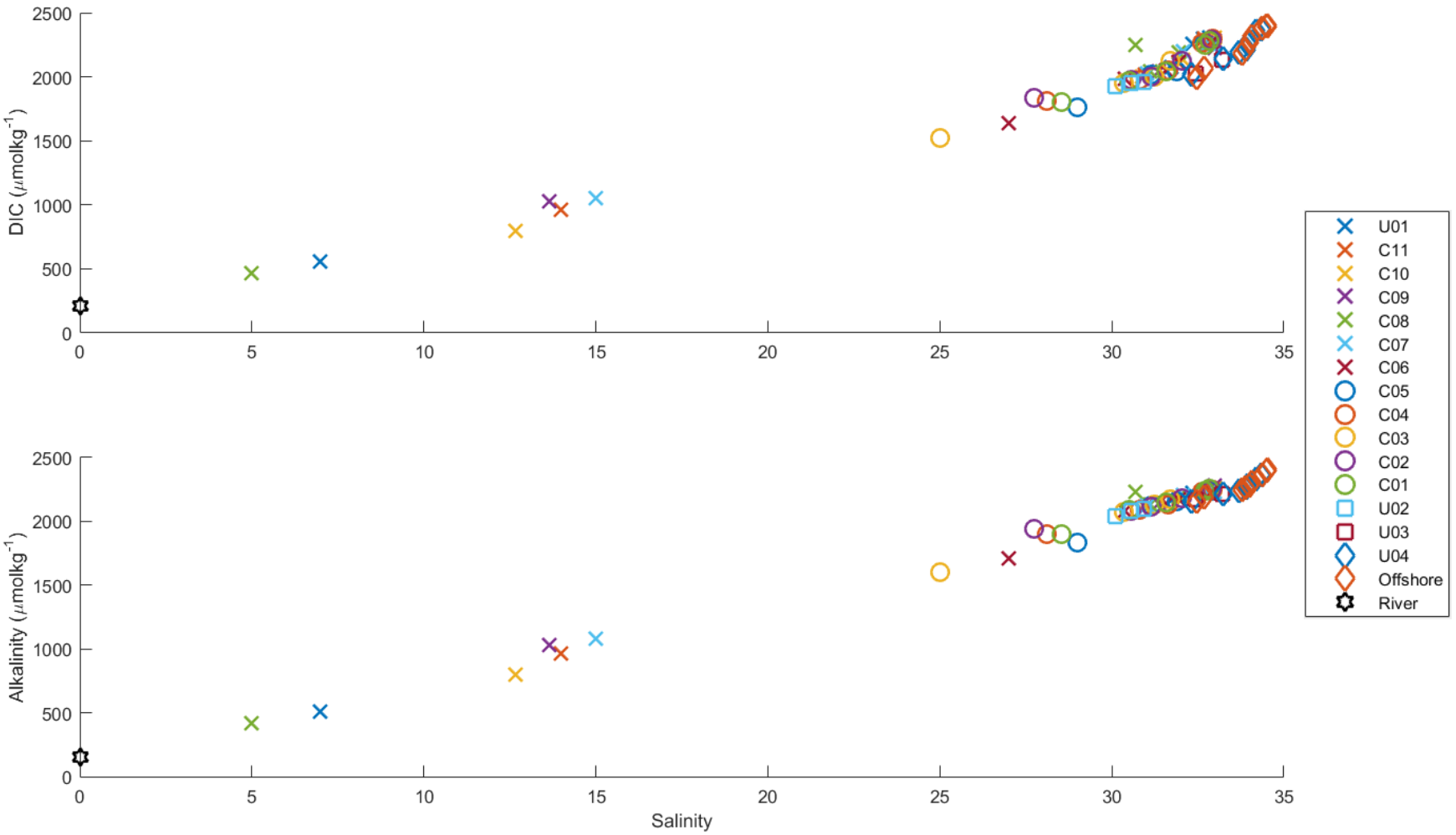

Figure 25 - DIC (top) and alkalinity (bottom) plotted against salinity. Shape and colour combination indicates station. X are used for stations within Muchalat Inlet, circles used for stations in within outer Nootka Sound area, squares for shelf stations, diamond for offshore/shelf edge stations.

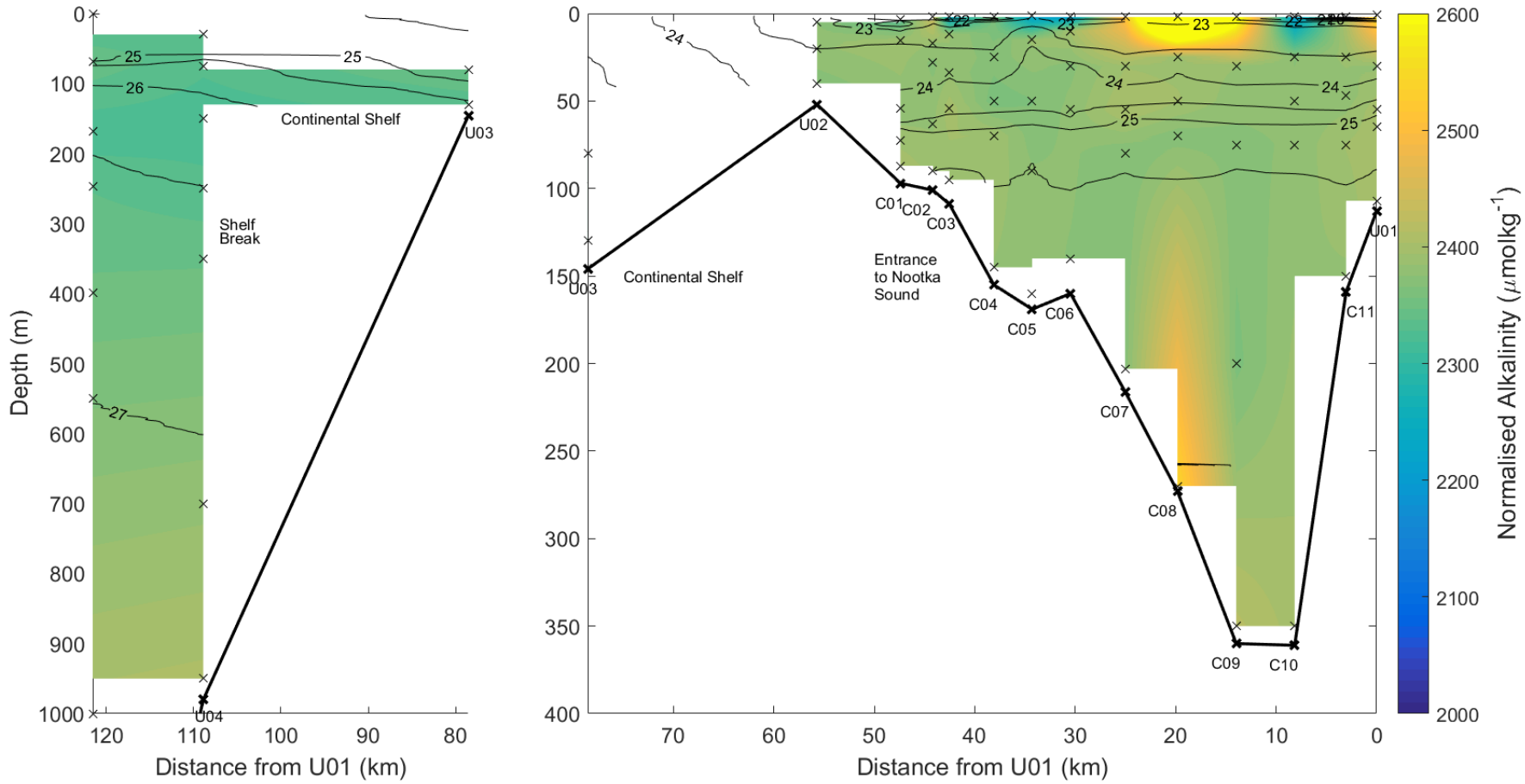

Figure 26 – Transect of alkalinity, normalised to a salinity of 35, from the head of Muchalat Inlet (right) to 60km offshore. Colour represents concentration, black lines are isopycnals of 0.5kgm^{-3} (density-1000), crosses mark locations where bottle data was taken, and thick black line represents each station depth with a line drawn between each station depth.

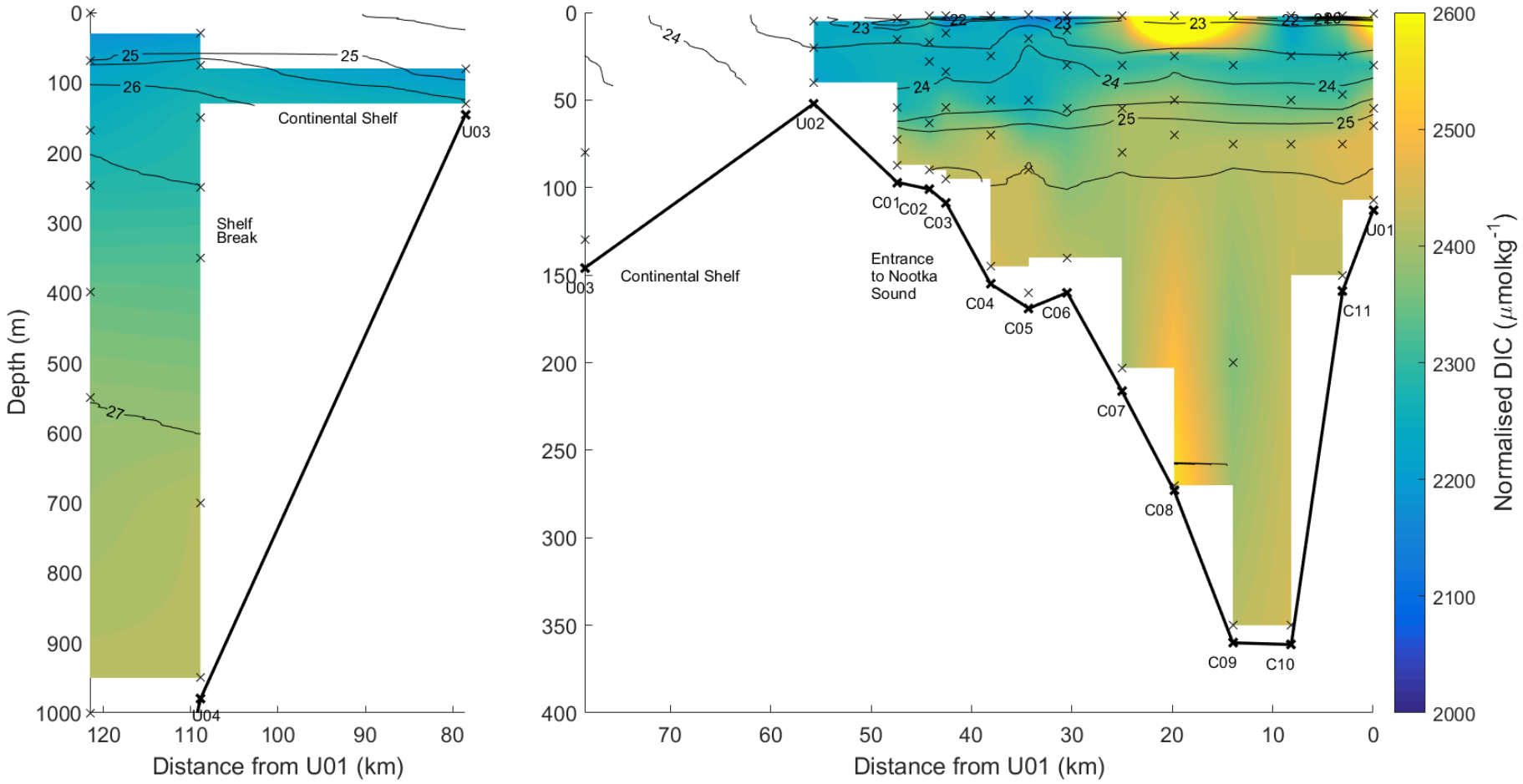

Figure 27 – Transect of dissolved inorganic carbon (DIC), normalised to a salinity of 35, from the head of Muchalat Inlet (right) to 60km offshore. Colour represents concentration, black lines are isopycnals of 0.5kgm^{-3} (density-1000), crosses mark locations where bottle data was taken, and thick black line represents each station depth with a line drawn between each station depth. Colour contour restricted to a maximum of 2600µmolkg^{-1}.